

Balancing long-range interactions and quantum pressure: Solitons in the Hamiltonian mean-field model

Ryan Plestid^{1,2,*} and D. H. J. O'Dell^{1,†}

¹*Department of Physics and Astronomy, McMaster University, 1280 Main St. W., Hamilton, Ontario, Canada L8S 4M1*

²*Perimeter Institute for Theoretical Physics, 31 Caroline St. N., Waterloo, Ontario, Canada N2L 2Y5*



(Received 9 May 2019; revised manuscript received 25 July 2019; published 19 August 2019)

The Hamiltonian mean-field (HMF) model describes particles on a ring interacting via a cosine interaction, or equivalently, rotors coupled by infinite-range XY interactions. Conceived as a generic statistical mechanical model for long-range interactions such as gravity (of which the cosine is the first Fourier component), it has recently been used to account for self-organization in experiments on cold atoms with long-range optically mediated interactions. The significance of the HMF model lies in its ability to capture the universal effects of long-range interactions and yet be exactly solvable in the canonical ensemble. In this work we consider the quantum version of the HMF model in one dimension and provide a classification of all possible stationary solutions of its generalized Gross-Pitaevskii equation (GGPE), which is both nonlinear and nonlocal. The exact solutions are Mathieu functions that obey a nonlinear relation between the wave function and the depth of the mean-field potential, and we identify them as bright solitons. Using a Galilean transformation these solutions can be boosted to finite velocity and are increasingly localized as the mean-field potential becomes deeper. In contrast to the usual local GPE, the HMF case features a tower of solitons, each with a different number of nodes. Our results suggest that long-range interactions support solitary waves in a novel manner relative to the short-range case.

DOI: [10.1103/PhysRevE.100.022216](https://doi.org/10.1103/PhysRevE.100.022216)

I. INTRODUCTION

Solitary waves are one of the most distinctive consequences of nonlinearity and result from a balance between dispersion and nonlinear forces. Their defining property is shape-preserving (i.e., dispersionless) propagation, as first noted in 1834 by J. Scott Russell when he observed them on the Edinburgh and Glasgow Union Canal [1]. The phenomenon has subsequently been extensively studied in classical hydrodynamics [2–5] and also in light propagating in optical fibers [6–11] and Bose-Einstein condensates (BECs) formed in dilute atomic gases. In the latter case, quantum pressure (quantum zero point motion) provides the stabilizing dispersion against collapse. Bright [12–17], dark [18–25], and dark-bright [26,27] varieties of solitary wave have all been observed in BECs.

In integrable systems solitary waves are guaranteed to survive collisions with one another, and are then referred to as *solitons*, i.e., elastically scattering and shape-preserving wave packets. Well-known examples occur in the Korteweg-de Vries equation [28–30], Sine-Gordon equation [28,29,31], and the nonlinear Schrödinger or Gross-Pitaevskii equation (GPE) [29,30,32]. The nonlinearity in all these wave equations appears as a local term that depends only on the wave function at the same point. For example, the GPE has a cubic term $g\Psi(\mathbf{x}, t)|\Psi(\mathbf{x}, t)|^2$ where g parameterizes the sign and magnitude of the self-coupling. However, there exist physical systems where long-range interactions (LRIs) lead to

a *nonlocal* nonlinearity that can also support solitary waves. This is the case in nonneutral plasmas [33], where there is a net Coulomb $1/r$ interaction, in the Calogero-Sutherland (CS) model [34–36], where particles interact via a $1/r^2$ potential, and in dipolar BECs [37–44], where dipole-dipole interactions lead to $1/r^3$ interactions. Nonlocal interactions also occur in optical systems, such as those mediated by thermal conduction [45–49], and their consequences have been observed experimentally [50,51]. The CS model is integrable and hence supports true solitons [52–55], whereas nonneutral plasmas are not integrable systems and only support solitary waves. Dipolar BECs display an instability where the attractive part of the interaction can cause the system to collapse [40]; far from the instability solitary waves are predicted to collide elastically and thus behave as solitons, whereas close to the instability the collisions become inelastic due to the emission of phonons [56]. In the BEC literature it is common not to distinguish solitons from solitary waves and thus we use the terms somewhat interchangeably in this paper.

In dipolar BECs solitons are usually analyzed using a generalized Gross-Pitaevskii equation (GGPE), which is an integro-differential equation that incorporates the nonlocal nonlinearity through a Hartree-type mean-field term of the form $\Psi(\mathbf{x}, t) \int V(\mathbf{x} - \mathbf{x}') |\Psi(\mathbf{x}', t)|^2 d\mathbf{x}'$ [56–61]. This approach has recently been put on a rigorous mathematical footing [62,63]; for reviews of nonlocal nonlinear Schrödinger equations we refer the reader to Refs. [64] and [65]. It has also been suggested that the Manakov equations [66] (which describe both two-component BECs [67] and randomly birefringent light in optical fibers [68,69]) can give rise to a so-called algebraic nonlinearity provided the system is prepared

*plestird@mcmaster.ca

†dodell@mcmaster.ca

with a specific set of initial conditions [70]. Integral terms can also appear in the equations describing the motion of vortices in superfluids at finite temperatures; they arise, for example, from the mutual friction between a solitary wave along a vortex and its surrounding flow [71].

Another physically important class of nonlocal nonlinearity is found in self-gravitating systems. In particular, compact yet stable astrophysical objects made of bosons and known as “Bose stars” have been hypothesized [72,73]. These can be identified as solitons if the attraction due to gravity is balanced by quantum pressure [74]. The realization that dark matter in the universe may be bosonic and cold enough to Bose condense into such Bose stars has driven considerable interest in these systems [75–81]. For the most part these studies use the nonrelativistic Schrödinger-Newton (also known as the Schrödinger-Poisson) equations [82,83], which result in a GGPE similar in form to both the GGPE used for dipolar BECs and also the equation to be studied in this paper. We also note in passing that laboratory analogues of the Schrödinger-Newton system have been proposed in the form of atomic BECs with a $1/r$ interaction provided by laser-induced dipole-dipole interactions [84,85].

The focus of the present paper is the Hamiltonian mean-field (HMF) model [86] which describes N particles of mass m living on a ring. They have positions $\theta_i \in (-\pi, \pi]$, angular momenta L_i , and interact via a pairwise cosine potential of strength ϵ giving the Hamiltonian

$$H = \sum_i \frac{L_i^2}{2I} + \frac{\epsilon}{N} \sum_{i<j} \cos(\theta_i - \theta_j), \quad (1)$$

where $I = mR^2$ is the moment of inertia for a ring of radius R . Since every particle interacts with every other due to the long-range nature of the interactions, a factor of $1/N$ is explicitly included to make the energy extensive (often termed the Kac prescription [87]). The cosine potential can be thought of as the first nonconstant term in a Fourier series expansion of a gravity- or Coulomb-like $1/r$ interaction around the ring, but without the singularity at $r = 0$ that otherwise complicates the treatment of such potentials. Another way to view the HMF model is as a system of N rotors interacting via an infinite range XY interaction. If $\epsilon > 0$ the particle interactions are repulsive at small distances, or equivalently, the rotors experience an antiferromagnetic coupling and hence prefer to antialign. If instead $\epsilon < 0$ the interactions are attractive-ferromagnetic and the rotors prefer to align. The average magnetization of the rotors along an axis specified by its angle φ to the vertical is given by $\langle \cos(\theta - \varphi) \rangle = (1/N) \sum_i \cos(\theta_i - \varphi)$, and this quantity serves as an order parameter for a symmetry-breaking phase transition (clustering transition) which occurs in the attractive case at low temperatures [88]. In this paper we focus on the attractive-ferromagnetic case.

The HMF model was originally written as a toy model, and its significance lies in the fact that it is simple and yet able to capture many of the general qualitative properties of systems with LRI; for reviews see Refs. [88–90]. However, more recently it was realized that cold atomic gases trapped in high-finesse optical cavities can directly realize the HMF

model [up to an additional term of the form $\cos(\theta_i + \theta_j)$] [91]. Here the long-range interactions are electromagnetic in origin and mediated by optical cavity modes that can extend over the entire gas. Ongoing experiments [92–97], many with BECs, have demonstrated symmetry breaking and self-organization in the atomic density distribution that is described by the HMF model [91,98–101].

One of the most striking properties of systems with LRI has long been appreciated by the astrophysics community: the two-body relaxation time (also known as the Chandrasekhar relaxation time) to thermodynamic (Boltzmann-Gibbs) equilibrium, diverges with the number of particles $t_{\text{relax}} \sim N t_{\text{cross}} / 10 \log[N]$, where t_{cross} is the typical time for a particle to cross the system [102]. Thus, in the thermodynamic limit $N \rightarrow \infty$ the system never achieves thermodynamic equilibrium. Nevertheless, when a self-gravitating system is disturbed from equilibrium the common mean-field potential that arises from the long-range nature of gravity becomes time dependent and can drive a rapid, collisionless relaxation mechanism known as violent relaxation whose timescale does not depend on the number of particles. This efficiently mixes phase space [102], but the process is nonergodic and the resulting quasistationary state is not the equilibrium state predicted by the microcanonical ensemble. However, coarse graining of the phase space distribution function by a macroscopic observer averages over the increasingly fine structures that develop during collisionless relaxation and in this way conventional statistical mechanics approaches can be applied [90,103–105]. The HMF model has been shown to display violent relaxation [106–109], as well as other generic consequences of LRI, including spontaneous symmetry breaking in low dimensions, i.e., the clustering phase transition mentioned above (LRI violate the Mermin-Wagner theorem), and the so-called “core-halo” statistics observed at late times in gravitational dynamics simulations [90,104,105].

The HMF model can be extended to describe quantum systems with LRI if we replace the kinetic energy term in Eq. (1) by its quantum operator $-\frac{\hbar^2}{2mR^2} \partial_{\theta_i}^2$, and the system is then equivalent to an infinite range $O(2)$ quantum rotor model [110–114]. Motivation for studying the quantum problem comes both from cold atom experiments and the Bose star picture of dark matter mentioned above. The equilibrium states of the quantum HMF model have been examined in Refs. [115,116] and the dynamics, including violent relaxation, were recently studied in Ref. [117], where it was found that the automatic coarse graining of phase space at the level of Planck’s constant \hbar can strongly modify the relaxation in the deep quantum regime. Furthermore, in its quantum form the HMF model bears a resemblance to the CS model mentioned above, which, when defined on a finite domain with periodic boundary conditions, has a pairwise interaction $V(\theta_i - \theta_j) = 1/\sin^2(\theta_i - \theta_j)$. Like the HMF model, the CS model has a periodic infinite range interaction. This connection is relevant in the present context because the CS model supports true solitons. The HMF model is not thought to be exactly integrable, but intriguingly, classical long-range interacting many-body systems are known to be described (exactly in the $N \rightarrow \infty$ limit [118]) by the Vlasov equation. Vlasov

dynamics *are integrable* for a on-dimensional system [119], such as the HMF model.¹ Furthermore, the classical (i.e., $\hbar \rightarrow 0$) limit of the GGPE corresponds to the “zero-temperature” limit of the Vlasov equation [108,109,117]. Therefore, although the HMF model is not exactly integrable, its classical dynamics are nearly integrable due to the structure of the Vlasov equation. We speculate that the “pseudo-integrability” extends also to the GGPE and may allow the solitary waves (bright solitons) presented here to scatter elastically.

Our goal in this work is to study solitary waves in the quantum HMF model with attractive-ferromagnetic interactions. We focus on the model’s associated GGPE, appropriate for describing the dynamics of a Bose condensed state (the HMF model, despite its name, describes a many-body system: to obtain a GGPE we assume all the particles occupy the same quantum state). We find that the exact solutions to this equation are Mathieu functions that satisfy a nonlinear self-consistency relation. As the interaction strength tends to infinity the number of these solutions also becomes infinite and we identify them as bright solitons each with a different number of nodes. Both the large number of solutions and the fact they have nodes makes them unusual when compared to the standard local GPE case [32]. We attribute these differences to the LRI themselves and hypothesize that this might be a generic feature.

This paper is organized as follows: In Sec. II we introduce the GGPE for the HMF model. In Sec. III we show how to find the full set of exact stationary solutions to the GGPE via a self-consistent Mathieu equation, and in Sec. IV we boost these solutions to finite velocity to obtain traveling waves. In Sec. V we explore the regime in which the solutions can be considered as bright solitons and discuss the parametric dependence of the stationary solutions on Planck’s constant. Next we discuss the asymptotic behavior of these solutions and derive useful analytic expressions. In Sec. VI we study their stability at leading order in the strong coupling regime by linearizing the equations of motion and analyzing the mode spectrum. Finally, in Sec. VII we summarize our work and discuss future directions of investigation.

II. GENERALIZED GROSS-PITAEVSKII EQUATION

An atomic BEC with short-range interactions is described by the standard GPE with a local cubic nonlinearity [121]

$$i\hbar \frac{\partial \Psi}{\partial t} = \left[-\frac{\hbar^2}{2m} \nabla^2 + V_{\text{ext}}(\mathbf{x}) + gN|\Psi|^2 \right] \Psi, \quad (2)$$

where N is the number of atoms, $\Psi(\mathbf{x}, t)$ is the condensate wave function normalized to unity: $\int_{-\infty}^{\infty} |\Psi|^2 d\mathbf{x} = 1$, $V_{\text{ext}}(\mathbf{x})$ is a possible external potential, e.g., a harmonic trap or periodic optical lattice potential, and the coupling constant g parameterizes the interatomic interactions (usually of the van der Waals type). Any stationary solution to this equation can be found in the usual way by putting $\Psi(\mathbf{x}, t) =$

$\psi(\mathbf{x}) \exp[-i\mu t/\hbar]$, giving

$$\mu \psi = \left[-\frac{\hbar^2}{2m} \nabla^2 + V_{\text{ext}}(\mathbf{x}) + gN|\psi|^2 \right] \psi. \quad (3)$$

If this were a linear Schrödinger equation, the eigenvalue μ would be the energy E of the state ψ . However, due to the nonlinearity of the GPE μ is in fact the chemical potential which is the change in energy associated with adding a particle to the system: $\mu = \partial E / \partial N$ [121]. In a waveguide configuration, where the BEC is tightly trapped in the x and y directions but untrapped along the z direction, the problem becomes effectively one-dimensional. Specializing further to the case of attractive interactions ($g < 0$), the stationary GPE has the bright soliton solution

$$\psi_0(z) = \psi_0(0) \frac{1}{\cosh(z/\sqrt{2\xi})}, \quad (4)$$

where $\rho_0 = |\psi_0(0)|^2$ is the central density and $\xi = 1/\sqrt{2m|g|\rho_0}$ is a characteristic length called the healing length [121]. In the optical soliton literature this solution is called the *fundamental soliton* and the coordinate z is replaced by $z - vt$ representing a shape-preserving waveform propagating at the group velocity v (there is also a multiplicative phase factor we shall not specify here) [11].

By contrast, the LRI in the HMF model lead to a *nonlocal nonlinearity* [116,117]. The HMF model lives on a ring so that the wave function obeys periodic boundary conditions $\Psi(\theta, t) = \Psi(\theta + 2\pi, t)$, and it also does not include an explicit potential $V_{\text{ext}}(\mathbf{x})$. Fixing the interactions to be attractive (i.e., $\epsilon < 0$), the HMF model’s GGPE can be written in reduced variables as

$$i\chi \frac{\partial \Psi}{\partial \tau} = \left[-\frac{\chi^2}{2} \frac{\partial^2}{\partial \theta^2} - \Phi(\theta, \tau) \right] \Psi, \quad (5a)$$

$$\text{where } \Phi(\theta, \tau) = \int_{-\pi}^{\pi} \rho(\theta', \tau) \cos(\theta - \theta') d\theta' \quad (5b)$$

is a nonlocal Hartree potential that depends on the integral over the angular probability density $\rho(\theta, \tau) = |\Psi(\theta, \tau)|^2$. We have introduced the quantities $\tau = t \times \sqrt{\frac{|\epsilon|}{mR^2}}$ and χ , the latter of which plays the role of a dimensionless Planck’s constant:

$$\chi = \frac{\hbar}{\sqrt{mR^2|\epsilon|}}. \quad (6)$$

Note that χ depends on the magnitude of the interaction strength $|\epsilon|$.

The seemingly complicated integro-differential equation given in Eq. (5) can be simplified by expanding the probability density in its Fourier components $\rho(\theta') = \sum \hat{\rho}_k e^{ik\theta'} / 2\pi$. We see that Φ depends only on $\hat{\rho}_{\pm 1}$, which we can write in all generality as $\hat{\rho}_{\pm 1} := M(\tau) \exp[\mp i\varphi(\tau)]$. From this it follows that the Hartree potential takes the remarkably simple form

$$\Phi(\theta, \tau) = M(\tau) \cos[\theta - \varphi(\tau)]. \quad (7)$$

The physical significance of this result is that all the individual two-body XY potentials of the many-body theory are replaced in the Gross-Pitaevskii theory by a single collective potential $\Phi(\theta, \tau)$ which retains the same XY form (a cosine) but breaks the angular symmetry by picking out a particular direction

¹Furthermore, the infinite set of Casimir invariants for the Vlasov equation can mimic the effects of integrability for higher dimensional systems with LRI; see, e.g., Ref. [120].

specified by $\varphi(\tau)$ along which the magnetization is $M(\tau)$. Furthermore, because $M(\tau)$ is the coefficient of the ± 1 terms in the Fourier expansion of the probability density, we can always project it out from the angular probability distribution via the integral

$$M(\tau) = \int_{-\pi}^{\pi} \rho(\theta, \tau) \cos(\theta - \varphi) d\theta, \quad (8)$$

which is the continuous version of the definition of the magnetization given in the Introduction, $M = \langle \cos(\theta - \varphi) \rangle = (1/N) \sum_i \cos(\theta_i - \varphi)$.

The stationary states $\Psi(\theta, \tau) = \psi(\theta) \exp[-i\mu\tau/\chi]$ of the GGPE satisfy the equation

$$-\frac{\chi^2}{2} \frac{\partial^2 \psi}{\partial \theta^2} + (-\mu - M[\psi] \cos \theta) \psi = 0, \quad (9)$$

where we have taken advantage of the fact that in the stationary case we can define our coordinates such that $\varphi = 0$. As for the case of contact interactions, the eigenvalue μ is not the same as the energy $E = \langle \psi | H | \psi \rangle$ of the state ψ associated with Hamiltonian given in Eq. (1), but is the chemical potential.

The stationary GGPE given in Eq. (9) has the same form as the Mathieu equation [122]

$$\frac{\partial^2 w}{\partial z^2} + [a - 2q \cos(2z)] w = 0, \quad (10)$$

whose solutions are Mathieu functions. These are denoted $ce_n(z; q)$ and $se_n(z; q)$ and have eigenvalues $a = A_n(q)$ and $B_n(q)$, respectively. In general, Mathieu functions also depend on a second parameter, which physically is the quasimomentum. However, here the quasimomentum is fixed to be zero by the periodic boundary conditions imposed by the ring.

There is a crucial difference between the standard Mathieu equation and the GGPE. Whereas the former corresponds to a linear problem where the ‘‘depth parameter’’ q of the cosine potential takes a fixed specified value, in our problem the depth of the cosine potential is the magnetization $M[\psi]$ which is a functional of the wave function and so depends on the solution itself. In other words, we have a nonlinear eigenvalue problem which, remarkably, has eigenvectors that are Mathieu functions obeying a linear equation but which must be supplemented by the self-consistency condition

$$M[\psi] = \int_{-\pi}^{\pi} |\psi(\theta')|^2 \cos(\theta') d\theta'. \quad (11)$$

We note that this is simply a restatement of Eq. (8) for a density $\rho(\theta) = |\psi(\theta)|^2$ that is independent of time.

An analogous situation occurs in cavity-QED where atoms are trapped in an optical cavity pumped by a laser [123–128]. The laser light forms a standing (or traveling [129,130]) wave inside the cavity which the atoms experience as a sinusoidal potential via the optical dipole interaction. The atoms’ center-of-mass wave function is therefore also determined by the Mathieu equation. However, the interaction acts back on the light which sees the atoms as a refractive medium. This backaction shifts the cavity’s resonance frequency, and hence controls the amount of laser light that can enter the cavity, by an amount that depends on the overlap between the atomic density distribution and the optical mode. In this way the

atomic density profile affects the depth of the sinusoidal potential which in turn affects the atomic density profile. The problem is therefore nonlinear and also leads to a Mathieu equation with a parameter q that must be determined self-consistently from the atomic wave function like in Eq. (11). One effect of this nonlinearity is the appearance of curious loops in the band structure that are not present in the linear problem and which can lie in the band gaps [124,131].

Band gap loops also occur in the problem of a BEC in an optical lattice of fixed depth, i.e., Eq. (2) with $V_{\text{ext}}(x) = V_0 \cos(kx)$, where the nonlinearity comes purely from interatomic interactions modeled by the cubic nonlinearity. This situation has been investigated both experimentally [132] and theoretically [133–138] where it is found that the loops correspond to two different types of solutions: periodic trains of solitons, i.e., spatially extended solutions [136,138], and localized band gap solitons [137]. Despite their localization, these latter solitons can have one or more nodes. In the HMF problem we also have a cosine potential but it is limited to a single period by the periodicity of the ring. This fixes the quasimomentum to zero and hence collapses the band structure to the center of the Brillouin zone. Still, we shall find analogous solutions to localized band gap solitons as will be described below.

III. SELF-CONSISTENT MATHIEU FUNCTIONS

To convert between the GGPE given in Eq. (9) and the standard form of the Mathieu equation given in Eq. (10) we make the identifications² $\theta = 2(z + \pi/2)$ and $\partial_z^2 = 4\partial_\theta^2$. Multiplying both sides of Eq. (10) by a factor of $-\chi^2/8$ we find

$$\mu = \frac{\chi^2}{8} a \quad \text{and} \quad M = \frac{\chi^2}{4} q. \quad (12)$$

The solutions we require are the ones that are 2π -periodic in the angle θ , and these correspond to ce_{2n} and se_{2n} with $n \geq 0$ an integer.

To find self-consistent solutions of the GGPE we use the following algorithm:

(1) We first treat q as a fixed parameter like in the usual linear theory of Mathieu functions. Taking a given Mathieu function of fixed n and q (which we denote q_n) we compute $M(q_n)$ using Eq. (11) where $\psi = ce_n(z; q_n)/\sqrt{\pi}$ or $\psi = se_{n+1}(z; q_n)/\sqrt{\pi}$ and $z = (\theta - \pi)/2$.

(2) Next, we obtain $\chi(q_n)$ by using Eq. (12), which gives $\chi(q_n) = \sqrt{4M(q_n)/q_n}$.

(3) The above two steps are repeated a large number of times for different values of q to obtain a map between χ and q . This must be done separately for each Mathieu function (each value of n).

(4) Although we have treated q as a parameter upon which χ depends, in reality the situation is reversed with q_n being determined self-consistently in terms of χ . We therefore invert the map $\chi(q_n)$ to find $q_n(\chi; \mathbb{N})$ where we have introduced the

²The shift in coordinates is equivalent to a negative value of q and accounts for the attractive nature of the interparticle interaction.

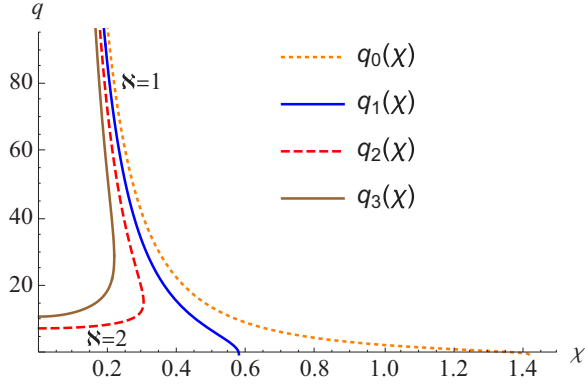


FIG. 1. Self-consistent values of the potential depth, as parameterized by q , as a function of χ for the first four stationary solutions: this plot shows which Mathieu functions satisfy both Eq. (9) and the self-consistency condition (11). Using Eq. (13) we can then find explicit expressions for the stationary state $\psi_n(\theta; \chi, \aleph)$. The parameter \aleph labels the different branches of $q_n(\chi; \aleph)$. Note that both $n = 2$ and $n = 3$ have two branches as the function turns back on itself. This is a generic feature for $n \geq 2$.

integer \aleph to label different branches of the function in the case that $\chi(q_n)$ is not invertible. The results are shown in Fig. 1.

Noting that Mathieu functions are conventionally normalized on the unit circle such that $\int |ce_n(\theta)|^2 d\theta = \pi$, and $\int |se_n(\theta)|^2 d\theta = \pi$, we define our stationary states as

$$\psi_n(\theta; \chi, \aleph) = \frac{1}{\sqrt{\pi}} \begin{cases} ce_n\left[\frac{\theta-\pi}{2}; q_n(\chi; \aleph)\right] & n \text{ even} \\ se_{n+1}\left[\frac{\theta-\pi}{2}; q_n(\chi; \aleph)\right] & n \text{ odd} \end{cases} \quad (13)$$

where $q_n(\chi; \aleph)$ is obtained via the algorithm outlined above. In Figs. 2 and 3 we plot some examples of these stationary solutions for $\chi = 0.5$ and $\chi = 0.05$, respectively, where in the latter case both branches of solutions exist, so we have chosen the $\aleph = 1$ branch. We see that n gives the number of nodes.

According to its definition in Eq. (6), χ decreases as the magnitude of the (attractive) interaction strength $|\epsilon|$ increases, and hence the $\aleph = 1$ branch solutions correspond most naturally to bright solitons: from Fig. 1 we see that as χ decreases the potential, as parameterized by q , becomes deeper and the states are more tightly bound as can be seen by comparing Fig. 2 with 3 (see Sec. V for further justification that these are really localized solutions). By contrast, the $\aleph = 2$ branch corresponds to shallower potentials which vary only slightly with χ . This branch continuously passes to negative χ (not shown in Fig. 3) corresponding to repulsive interactions, which shows that the repulsive HMF model can also support stationary states; however, we emphasize that these states

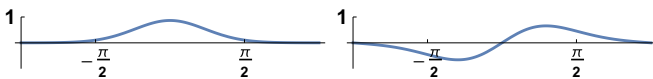


FIG. 2. Plots of the two self-consistent stationary solutions to the GGPE [Eqs. (5a) and (5b)] that exist at $\chi = 0.5$. They are the $n = 0$ and $n = 1$ states, where n gives the number of modes. The solutions are periodic with period 2π .

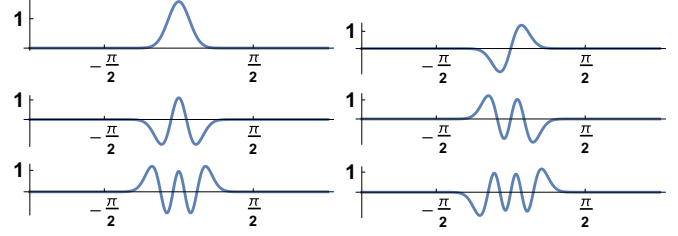


FIG. 3. Plots of the first six self-consistent stationary solutions to the GGPE for $\chi = 0.05$. These solutions all lie on the upper branch of Fig. 1, i.e., $\psi_n(\theta; \chi, \aleph = 1)$ where $n \in \{0, 1, 2, 3, 4, 5\}$. Note that even for moderately small values of χ the first few stationary states are quite well localized, and upon a Galilean transformation to finite velocity can be interpreted as solitary wave solutions. All states are periodic with period 2π .

generally have smaller values of q and are less localized than their attractive interacting counterparts.

The first two solutions, ψ_0 and ψ_1 , have only a single branch and are shown in Fig. 2. For weak interactions ($\chi \gg 1$) one finds that q is zero so that the self-consistent Hartree cosine potential is zero. These solutions then correspond to ordinary sine waves (although, as shown in Fig. 4, for $\chi > \sqrt{2}$ the energy eigenvalue or chemical potential corresponding to ψ_0 takes the value $\mu = 0$, and thus this is a trivial solution corresponding to an infinite wavelength, i.e., a flat density profile). However, at a critical value of χ , which is different for each solution, the Hartree potential switches on and the solutions evolve continuously into Mathieu functions. For ψ_0 this occurs at $\chi = \sqrt{2}$ [116], and for ψ_1 it occurs at $\chi = 1/\sqrt{3}$. The higher solutions behave differently, as can be seen from Fig. 1. In their case each solution again switches on below a critical value χ , but q takes on a finite value at the point each solution appears (and which immediately splits into two branches).

With the knowledge of the dependence of the q_n 's upon χ depicted in Fig. 1 we can straightforwardly obtain physical quantities such as the chemical potentials and magnetizations

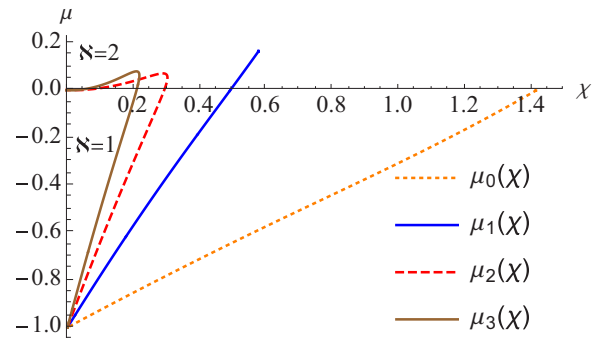


FIG. 4. The eigenvalues μ of the GGPE as a function of χ for the first four stationary solutions. μ_0 and μ_1 abruptly appear at critical values of $\chi = \sqrt{2}$ and $\chi = 1/\sqrt{3}$, respectively; for larger values of χ the self-consistent Hartree cosine potential is zero (i.e., $q = 0$), and the solutions ψ_0 and ψ_1 are ordinary sine waves so we have not plotted that portion of their eigenvalues. Like in Fig. 1, $\aleph = 1$ and $\aleph = 2$ label the two branches of the higher solutions.

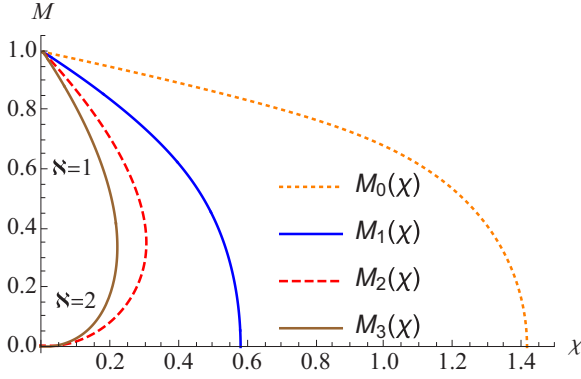


FIG. 5. The magnetization M as a function of χ for the first four stationary solutions. With the exception of the two lowest states, the solutions have two branches labeled by $\aleph = 1$ and $\aleph = 2$ like in the earlier figures. Treating the magnetization as an order parameter signifying a clustering or ordering phase transition which breaks the angular symmetry of the system, we see that this transition is second order (continuous), at least in the lowest two states. The fact that a phase transition occurs in a 1D system is a special feature of LRI.

of all the stationary states. These are plotted in Figs. 4 and 5, respectively. Each chemical potential $\mu_n = \partial E_n / \partial N$ gives the change in energy of its respective state $E_n = \langle \psi_n | H | \psi_n \rangle$ when a particle is added to the system. From Fig. 4 we see that the gaps between the different μ_n vanish linearly as $\chi \rightarrow 0$, so that all μ_n tend to the common value of -1 . However, the rate at which they approach this limit is higher the higher the state so that the largest gap is between μ_0 and μ_1 .

Although the chemical potential is sensitive to the clustering or ordering phase transition that occurs at the critical value of χ , it is the magnetization which is usually taken as the order parameter for the transition [88]. In particular, examining the behavior of the magnetization M_0 of the lowest state in Fig. 4, we see that when the coupling is weak ($\chi \gg 1$) the magnetization is zero but at the critical value $\chi = \sqrt{2}$ it begins to take on finite values indicating a second order (continuous) phase transition. Similar behavior is found for M_1 . However, the behavior of the magnetization of the higher states is more complicated; nevertheless the $\aleph = 1$ branches of these states, which correspond to bright solitons, tend to full magnetization $M = 1$ in the strong coupling regime $\chi \ll 1$.

The results given in this section generalize those obtained by Chavanis [116] for the ground state of the quantum HMF model. In particular, the approach described above allows one to classify *all possible* stationary states of the GGPE. They are labeled by their number of nodes n , and their depth parameter $q_n(\chi; \aleph)$. Furthermore, while the approach followed in Ref. [116] gives an expansion for the small q properties of the ground state $\psi_0(\theta; \chi)$, as well as the leading order result in the strong-coupling regime $\chi \ll 1$, the approach followed here is valid for all values of χ and, upon computation of $q_n(\chi)$, provides an analytic expression for $\psi_n(\theta)$. The standard large and small q asymptotics of the Mathieu functions [122] can then be used to obtain analytic approximations for $q_n(\chi; \aleph = 1)$.

The fact that the GGPE admits a tower of stationary solutions $\psi_n(\theta; \chi, \aleph)$, each labeled by its number of nodes n

and branch \aleph , is quite distinct from the case of the local GPE where there is only a single stationary bright soliton solution, i.e., the nodeless fundamental soliton given in Eq. (4). In particular, the GGPE’s tower of stationary solutions should not be confused with the so-called “higher order solitons” found in the local GPE which can display multiple peaks and nodes at certain instants of time [6, 11, 139]. These higher order solitons are time-dependent combinations of the fundamental and do not correspond to the individual stationary solutions we describe above. Indeed, as famously shown by Zakharov and Shabat [140], the inverse scattering transform method can be applied to the local GPE and in general gives rise to a nonlinear superposition of multiple fundamental solitons and continuous waves (see p. 21 in Ref. [9] and p. 245 in Ref. [11] for a summary of these results).

IV. BOOSTED SOLUTIONS

The same solutions as already described for the stationary case can be transformed to traveling waves with velocity v by performing a Galilean boost:

$$\psi_n(\theta) e^{-i\mu_n \tau / \chi} \rightarrow \psi_n(\theta - v\tau) e^{iv\theta / \chi} e^{-i(\mu_n + v^2/2)\tau / \chi}. \quad (14)$$

In order that these wave functions still satisfy the periodic boundary conditions we require that $v/\chi = n$ with $n \in \mathbb{Z}$. The existence and classification of these wave functions is the main result of our work. In the next section we will see when they can be considered to be solitary waves.

V. EMERGENCE OF SOLITONS AT STRONG COUPLING

Having established the existence of nontrivial stationary and traveling waves we will now argue that the crucial solitonic property of localization emerges in the strong-coupling regime $\chi \ll 1$. Finally, we show how in this same limit an explicit asymptotic series for the depth parameter $q_n(\chi)$ can be obtained.

A. Localization in the strong-coupling regime

In the limit of strong coupling the Hartree mean-field potential is deep relative to the kinetic energy, and the magnetization can be expected to saturate to unity. It then follows via the relation $q = 4M/\chi^2$ that this limit corresponds to large values of q , and we will see that this is indeed the case.

As $q \rightarrow \infty$ the eigenvalues, A and B , of the Mathieu equation display the well-known asymptotic behavior as a function of q [122],

$$\left. \begin{matrix} A_n(q) \\ B_{n+1}(q) \end{matrix} \right\} \sim -2q \left[1 - \frac{1}{\sqrt{q}} (2n + 1) + O\left(\frac{1}{q}\right) \right], \quad (15)$$

from which we can identify that the low-lying states are bound within a deep well³ whose minimum is spontaneously chosen

³The spectrum is that of a harmonic oscillator with anharmonic corrections occurring at $O(1/q)$.

around the ring. There are two classical turning points:

$$\theta_{\text{turn}}^{\pm} \sim \pm \frac{(4n+2)^{1/2}}{q^{1/4}} + O\left(\frac{1}{q^{1/2}}\right). \quad (16)$$

At distances $|\theta| \gtrsim 2\theta_{\text{turn}}^+$ the wave function is exponentially suppressed and consequently the state is localized in a region around the mean-field potential's minimum (as can be seen in Fig. 3). The size of this region shrinks with q and shows that localized stationary states emerge in the strong-coupling regime, and, by Galilean invariance, so too do finite-velocity traveling solitons. Thus, we identify the solutions as solitary waves because they can be arbitrarily localized and their shape is determined by a competition between quantum dispersion and a classical mean-field potential, Φ , which is the source of the nonlinearity in Eq. (5).

We may quantify the regime in which soliton-like solutions appear by estimating a critical value $q_n^{(c)}$ above which the stationary state is sufficiently narrow to be considered localized relative to the spatial extent of the unit circle. Demanding that $\theta_{\text{turn}}^+ < \pi/4$ implies that for q satisfying

$$q \gtrsim q_c(n) = \frac{64}{\pi^4} (2n+1)^2 \approx \frac{2}{3} (2n+1)^2, \quad (17)$$

or equivalently⁴ for χ satisfying

$$\chi \lesssim \frac{\pi^2/8}{2n+1} \approx \frac{1.23}{2n+1}, \quad (18)$$

the stationary states discussed above are well localized.

From Eq. (16) we see that for fixed n the stationary states' widths tends to zero and are localized within an interval of size $\Delta\theta \sim O(1/q^{1/4})$ centered about the minimum of the mean-field potential. This suggests approximating the cosine potential as a quadratic potential well, and a thorough analysis reveals that this can be done provided the turning point structure of the problem is preserved. The stationary solutions in this regime are parabolic cylinder functions [141–144]:

$$\psi_n(\theta; q) \sim \left[\frac{\sqrt{q}}{2\pi(n!)} \right]^{1/4} \begin{cases} D_n(\zeta) & n \text{ even} \\ \cos(\frac{1}{2}\theta) D_n(\zeta) & n \text{ odd} \end{cases}, \quad (19)$$

where $\zeta = 2q^{1/4} \sin(\theta/2)$ [see Eqs. (A4) and (A5) for a more extensive discussion].

B. Magnetization and Hartree potential depth in the strong coupling regime

We seek to compute the magnetization

$$M(q_n) = \int_{-\pi}^{\pi} d\theta |\psi_n(\theta; q)|^2 \cos \theta \quad (20)$$

in the strong coupling regime. Expanding the wave function in terms of parabolic cylinder functions, and changing variables to $\zeta = 2q^{1/4} \sin(\theta/2)$, we obtain

$$M(q) = \int_{-2q^{1/4}}^{2q^{1/4}} \frac{d\zeta}{q^{1/4}} \left[\frac{1 - \frac{\zeta^2}{2\sqrt{q}}}{\sqrt{1 - \frac{\zeta^2}{4\sqrt{q}}}} \right] |\psi_n(\zeta; q)|^2. \quad (21)$$

A Taylor expansion of $(1 - \frac{\zeta^2}{2\sqrt{q}})/\sqrt{1 - \frac{\zeta^2}{4\sqrt{q}}}$ and knowledge of integrals of the form

$$I_{n,m}^{(k)} = \int_{-\infty}^{\infty} d\zeta D_n(\zeta) D_m(\zeta) \zeta^k \quad (22)$$

allows one to compute asymptotic expressions for the magnetization as a function of q , the details of which can be found in Appendix A. We find

$$M(q_n) \sim 1 - \frac{1}{\sqrt{q}} \left[\frac{2n+1}{2} \right] + O\left(\frac{1}{q^{3/2}}\right). \quad (23)$$

This equation applies to the branches of solutions labeled by $\aleph = 1$ in Fig. 1.

With this result we may now compute $\chi_n(q) = \sqrt{4M/q}$, which can subsequently be inverted yielding

$$q_n(\chi; \aleph = 1) \sim \frac{4}{\chi^2} \left[1 - \frac{2n+1}{4} \chi - \frac{(2n+1)^2}{32} \chi^2 \right], \quad (24)$$

where, again, $\aleph = 1$ denotes the branch of $q_n(\chi)$ to which our asymptotic analysis applies.

The above asymptotic analysis is only sensible provided that χ is sufficiently small such that dispersive effects are weak relative to the mean-field Hartree potential. Quantitatively we require that Eq. (18) is satisfied; for $n = 0$ and $n = 1$ this occurs for values of $\chi \lesssim 1$.

C. Energy in the strong coupling regime

An analytic expression for the energy of a solitary wave can also be obtained in the small- χ limit. The energy functional (i.e., Hamiltonian) for the HMF model is

$$\begin{aligned} \mathcal{E} &= \int \psi^* \left[-\frac{1}{2} \chi^2 \partial_{\theta}^2 \right] \psi d\theta - \frac{1}{2} M[\psi]^2 \\ &= \mu_n + \frac{1}{2} M[\psi_n]^2, \end{aligned} \quad (25)$$

where in the second equality we have used Eq. (9). The small- χ behavior of the magnetization M is given by Eqs. (23) and (24),

$$M \sim 1 - \frac{2n+1}{4} \chi, \quad (26)$$

while the chemical potential's behavior can be found by using the large- q asymptotics of $a_n \sim -2q + (4n+2)\sqrt{q}$, which, when written in terms of χ , gives

$$\begin{aligned} \mu_n &= \frac{\chi^2}{8} \times a_n \sim \frac{\chi^2}{2} [-2q(\chi) + (4n+2)\sqrt{q(\chi)}] \\ &\sim -1 + \frac{3}{4} (2n+1) \chi. \end{aligned} \quad (27)$$

Thus we have

$$\mathcal{E}_n \sim -\frac{1}{2} + \frac{2n+1}{4} \chi, \quad (28)$$

such that the energy increases linearly with n at leading order in χ ; a nonperturbative graph of the energy's n dependence can be obtained by combining the curves plotted in Figs. 4 and 5.

⁴Taking $M \sim O(1)$ as $q \rightarrow \infty$.

VI. LINEAR STABILITY ANALYSIS

In order to understand whether the solitary waves analyzed in the previous two sections are stable, we study their linearized equations of motion in the soliton's rest frame. Since we identify these solutions as being solitary waves in the limit that $\chi \rightarrow 0$, and since for $n \geq 2$ the solutions exist only for small values of χ , we restrict our analysis to the $\aleph = 1$ branch of solutions in the limit that $\chi \rightarrow 0$ such that a large- q expansion is justified.

We consider stability of the soliton solutions with respect to perturbations of the Bogoliubov form

$$\Psi(\theta, \tau) = [\psi_n(\theta) + \delta\psi_n(\theta, \tau)]e^{-i\mu\tau/\chi}, \quad (29)$$

$$\delta\psi_n(\theta, \tau) = \sum_{\alpha} U_{\alpha}(\theta)e^{-i\omega_{\alpha}\tau/\chi} + V_{\alpha}^*(\theta)e^{i\omega_{\alpha}^*\tau/\chi}, \quad (30)$$

which have real frequencies if the unperturbed solution is stable, and complex frequencies if it is dynamically unstable [32]. Substituting this ansatz into Eq. (5), working to first order in U_{α} and V_{α}^* , and collecting terms varying in time as $e^{-i\omega_{\alpha}\tau/\chi}$ and $e^{i\omega_{\alpha}^*\tau/\chi}$, respectively, one finds the following coupled equations for the normal modes:

$$\omega U(\theta) = (\widehat{H}_n - \mu_n)U(\theta) - \Phi(\theta)\psi_n(\theta), \quad (31)$$

$$-\omega V(\theta) = (\widehat{H}_n - \mu_n)V(\theta) - \Phi(\theta)\psi_n(\theta), \quad (32)$$

where we have used the reality of the soliton, $\psi_n^* = \psi_n$ (since we are in the rest frame of the solitary wave). The subscript α has been left implicit, $\widehat{H}_n = -\frac{1}{2}\chi^2\partial_{\theta}^2 - M[\psi_n]\cos\theta$, and we define the linearized mean-field potential as

$$\Phi(\theta) = \int_{-\pi}^{\pi} [U(\theta') + V(\theta')]\psi_n(\theta')\cos(\theta - \theta')d\theta'. \quad (33)$$

It is convenient to decompose both $U(\theta)$ and $V(\theta)$ in terms of the set of Mathieu functions orthogonal to ψ_n , which we will denote by $\{\phi_m\}$. Note that these solutions are complete and satisfy the linear equation

$$\widehat{H}_n\phi_m = -\frac{1}{2}\chi^2\phi_m'' + M[\psi_n]\cos(\theta)\phi_m = \lambda_m\phi_m, \quad (34)$$

where λ_m is related to the eigenvalue a_m of Eq. (10) via $\lambda_m = \chi^2 a_m/8$ [cf. Eq. (12)]. Importantly, $M[\psi_n]$ is the magnetization induced by the soliton solution ψ_n and is independent of ϕ_m . Explicitly, we have $U(\theta) = \sum_m u_m\phi_m(\theta)$ and $V(\theta) = \sum_m v_m\phi_m(\theta)$ where u_m and v_m are c-numbers and $m \neq n$. This final condition ensures that our linear operator is diagonalizable [145].

To find the frequencies $\{\omega_{\alpha}\}$, we take Eqs. (31) and (32) and operate on both sides with $\int d\theta\phi_m(\theta)$. By virtue of the orthogonality relations $\int \phi_m\phi_{\ell}d\theta = \delta_{m\ell}$ and $\int \phi_m\psi_n d\theta = 0$, this projects out the m th element of $\{\phi_m\}$ and allows us to express Eq. (31) in terms of the coefficients u_{ℓ} and v_{ℓ} via

$$\omega u_m = (\lambda_m - \mu_n)u_m - \sum_{\ell \neq n} F_{m\ell}(u_{\ell} + v_{\ell}), \quad (35a)$$

$$-\omega v_m = (\lambda_m - \mu_n)v_m - \sum_{\ell \neq n} F_{m\ell}(u_{\ell} + v_{\ell}), \quad (35b)$$

where the quantity $F_{m\ell}$ is defined as

$$F_{m\ell} = \mathcal{I}_{\ell,n}^C \mathcal{I}_{m,n}^C + \mathcal{I}_{\ell,n}^S \mathcal{I}_{m,n}^S, \quad (36)$$

and where the integrals $\mathcal{I}_{\ell,n}^C$ and $\mathcal{I}_{\ell,n}^S$ are defined in terms of the mean-field solutions via

$$\mathcal{I}_{m,n}^C = \int_{-\pi}^{\pi} \phi_m(\theta)\psi_n(\theta)\cos\theta d\theta, \quad (37a)$$

$$\mathcal{I}_{m,n}^S = \int_{-\pi}^{\pi} \phi_m(\theta)\psi_n(\theta)\sin\theta d\theta. \quad (37b)$$

We may interpret $F_{m\ell}$ as a matrix operator acting on the vector $(u + v)_{\ell}$ such that the equations can be cast in the form

$$\omega_n \begin{pmatrix} u \\ v \end{pmatrix} = \frac{1}{\sqrt{q}} \begin{pmatrix} \mathcal{D}_n - \mathcal{F}_n & -\mathcal{F}_n \\ \mathcal{F}_n & -(\mathcal{D}_n - \mathcal{F}_n) \end{pmatrix} \begin{pmatrix} u \\ v \end{pmatrix}. \quad (38)$$

Here \mathcal{D}_n is a diagonal matrix with $\mathcal{D}_n^{m,m} = \sqrt{q}(\lambda_m - \mu_n)$ along the diagonal, while the matrix elements of \mathcal{F} are related to those of F via $\mathcal{F}_{m\ell} = \sqrt{q}F_{m\ell}$. Physically, \mathcal{D}_n tells us whether an orthogonal Mathieu function ϕ_m has a larger or smaller eigenvalue (chemical potential) as compared to the soliton ψ_n . The matrix \mathcal{F}_n is the mode-to-mode coupling induced indirectly by the soliton.

Explicit expressions for the matrix elements $F_{m\ell}$ and $\mathcal{D}_n^{m,m}$ can be obtained in the large- q (i.e., small- χ) regime. As outlined in Appendix B, by making large- q expansions of the integrals $\mathcal{I}_{m,n}^C$ and $\mathcal{I}_{m,n}^S$, then at $O(1/\sqrt{q})$ only $\mathcal{I}_{m,n}^S$ contributes to $F_{m\ell}$ with the explicit (leading order) formula being

$$\mathcal{I}_{m,n}^S \sim \frac{1}{q^{1/4}}(\sqrt{n+1}\delta_{m,n+1} + \sqrt{n}\delta_{m,n-1}). \quad (39)$$

Higher order terms connect states with $m = n \pm 2$, $m = n \pm 3$, etc. Likewise, to find the large- q behavior of \mathcal{D}_n , we can use the large- q asymptotic formula for the eigenvalues of the Mathieu equation [122]:

$$\mu_n \sim \frac{\chi^2(q_n)}{8} \left\{ -2q + 2(2n+1)\sqrt{q} + \frac{1}{8}[(2n+1)^2 + 1] \right\}, \quad (40)$$

$$\lambda_m \sim \frac{\chi^2(q_n)}{8} \left\{ -2q + 2(2m+1)\sqrt{q} + \frac{1}{8}[(2m+1)^2 + 1] \right\}. \quad (41)$$

Notice that both λ_m and μ_n are multiplied by the same value of χ^2 , which corresponds to the soliton's self-consistent depth parameter q_n . At leading order this implies that $\mathcal{D}_n^{m,\ell} \sim 2(m-n)\delta_{\ell,m}$, and that all of \mathcal{F}_n 's nonvanishing entries are contained within a 2×2 block composed of $\ell, m = n \pm 1$ (unless $n = 0$) given by

$$\begin{pmatrix} n & \sqrt{n(n+1)} \\ \sqrt{n(n+1)} & n+1 \end{pmatrix}. \quad (42)$$

This implies that in the strong-coupling regime the perturbations about the soliton are *weakly interacting*, with the exception of the two Mathieu modes whose eigenvalues are closest to the soliton's chemical potential. These two modes actually couple with a strength that is $O(n)$ such that solitons with a higher number of nodes mediate stronger interactions than those with fewer nodes. By contrast, if $n = 0$ (i.e., if we are perturbing around the lowest energy soliton), then intermode coupling does not exist at $O(1/\sqrt{q})$ and \mathcal{F}_n is diagonal at leading order, having all vanishing entries except

for $\mathcal{F}_n^{11} = 1$. We focus now on $n \geq 1$ after which we will return to $n = 0$ as a special case.

By rewriting Eq. (38) in terms of $u + v$ and $u - v$, it can be easily seen that the eigenvalues of the above matrix equation are determined by the condition that

$$\text{Det}[q\omega_n^2 \mathbb{1} - (\mathcal{D}_n^2 - 2\mathcal{F}_n \mathcal{D}_n)] = 0. \quad (43)$$

The spectrum of $\mathcal{D}_n^2 - 2\mathcal{F}_n \mathcal{D}_n$ is the same as that of \mathcal{D}_n^2 except for the two eigenvalues that are determined (for $n \geq 1$) by the 2×2 matrix

$$\begin{pmatrix} 4n+4 & -4\sqrt{n(n+1)} \\ 4\sqrt{n(n+1)} & -4n \end{pmatrix}, \quad (44)$$

whose eigenvalues are independent of n and given by $\lambda_1 = 0$ and $\lambda_2 = 4$. We thereby find that the entire spectrum is positive, indicating stability, except for one entry which is marginal at this order, being neither positive nor negative.

To elucidate the stability of the mode corresponding to λ_1 we must calculate subdominant corrections to \mathcal{I}^S , and $\lambda_m - \mu_n$. This can be achieved using first-order perturbation theory for which we need the eigenvector corresponding to λ_1 at leading order, which is given by

$$v_1 = (\sqrt{n/(2n+1)}, \sqrt{(n+1)/(2n+1)})^T. \quad (45)$$

If we denote the subdominant corrections as $\delta\mathcal{D}_n$ and $\delta\mathcal{F}_n$ (such that $\mathcal{D}_n \rightarrow \mathcal{D}_n + q^{-1/2}\delta\mathcal{D}_n$ and $\mathcal{F}_n \rightarrow \mathcal{F}_n + q^{-1/2}\delta\mathcal{F}_n$) then, the first-order perturbative correction to the eigenvalue is given by

$$\lambda_1 \sim \frac{1}{\sqrt{q}} v_1^T [\{\mathcal{D}_n, \delta\mathcal{D}_n\} - 2(\delta\mathcal{F}_n \mathcal{D}_n + \mathcal{F}_n \delta\mathcal{D}_n)] v_1, \quad (46)$$

where the curly braces denote an anticommutator. Using Eqs. (40) and (41) we find for $\delta\mathcal{D}_n$

$$\delta\mathcal{D}_n = \begin{pmatrix} \frac{1}{4}(10n+4) & 0 \\ 0 & \frac{1}{4}(-6-10n) \end{pmatrix}. \quad (47)$$

The relevant matrix elements of \mathcal{F} are $\mathcal{F}_{\ell m}$ with $\ell, m = n \pm 1$ which can be represented as a 2×2 matrix

$$\delta\mathcal{F} = \begin{pmatrix} -\frac{3}{4}n^2 & -\frac{3}{8}\sqrt{n(n+1)}(2n+1) \\ -\frac{3}{8}\sqrt{n(n+1)}(2n+1) & -\frac{3}{4}(1+n)^2 \end{pmatrix} \quad (48)$$

such that

$$\lambda_1 \sim \frac{1}{\sqrt{q}} \times \frac{n(1+n)}{2n+1} \quad \text{for } n \geq 1. \quad (49)$$

Thus, for $n \geq 1$ all of the eigenvalues λ are positive definite, such that ω_m is always real, and the solitons are dynamically stable. The typical frequencies are given by $\omega_m \sim \frac{2}{\sqrt{q}} |m-n| \sim \chi |m-n|$, while the smallest frequency is parametrically smaller being given by $\omega_1 = \pm \sqrt{\lambda_1/q} \sim O(\chi^{3/2})$.

As mentioned above, the case of the $n = 0$ is different. Here the zeroth eigenvector is $v_1 = (1, 0)^T$, and it turns out that its eigenvalue is small $\lambda_1 \sim O(1/q)$. If we define the matrix $M = \mathcal{D}_n^2 - 2\mathcal{F}_n \mathcal{D}_n$, then we have that

$$M = \begin{pmatrix} M_{11} & 0 & M_{13} \\ 0 & M_{22} & 0 \\ M_{31} & 0 & M_{33} \end{pmatrix}, \quad (50)$$

where the zeros stem from the fact that $\mathcal{I}_{0,m}^C = 0$ if m is odd. As we will soon see, M_{13} and M_{31} are both $O(1/\sqrt{q})$ while M_{33} is $O(1)$, and we can therefore calculate the correction to λ_1 within second-order perturbation theory

$$\lambda_1 \sim M_{11} + \frac{M_{13}M_{31}}{M_{11} - M_{33}} + O(q^{-3/2}) \quad \text{for } n = 0. \quad (51)$$

Explicit formula for M_{11} , M_{13} , and M_{31} in terms of $\mathcal{I}_{0,m}^S$ and $\Delta_m = \lambda_m - \mu_0$ are given by

$$M_{11} = q\Delta_1^2 - 2q\Delta_1 \mathcal{I}_{0,1}^S \mathcal{I}_{0,1}^S, \quad (52)$$

$$M_{13} = -2q\Delta_3 \mathcal{I}_{0,1}^S \mathcal{I}_{0,3}^S, \quad (53)$$

$$M_{31} = -2q\Delta_1 \mathcal{I}_{0,1}^S \mathcal{I}_{0,3}^S, \quad (54)$$

$$M_{33} = q\Delta_3^2 - 2q\Delta_3 \mathcal{I}_{0,3}^S \mathcal{I}_{0,3}^S. \quad (55)$$

The large q behavior of Δ_m can be found by using Eq. (28.8.1) of Ref. [122] and the next-to-next-to leading order expression for $\chi(q_n)$ given in Eq. (A18). To compute $\mathcal{I}_{0,m}^S$ we make use of Eqs. (28.8.3) to (28.8.7) from [122] at next-to-next-to leading order accuracy. At the level of accuracy required to compute λ_1 the results are

$$q^{1/4} \mathcal{I}_{0,1}^S \sim 1 - \frac{3}{8\sqrt{q}} - \frac{19}{256q}, \quad (56)$$

$$q^{1/4} \mathcal{I}_{0,3}^S \sim -\frac{3\sqrt{3/2}}{8\sqrt{q}}, \quad (57)$$

$$\sqrt{q}\Delta_1 \sim 2 - \frac{3}{2\sqrt{q}} + \frac{3}{16q}, \quad (58)$$

$$\sqrt{q}\Delta_3 \sim 6. \quad (59)$$

Substituting these expressions into Eqs. (52) to (55) we find

$$M_{11} \sim \frac{13}{32q} + O\left(\frac{1}{q^{3/2}}\right), \quad (60)$$

$$M_{13} \sim \frac{9\sqrt{3/2}}{2\sqrt{q}} + O\left(\frac{1}{q}\right), \quad (61)$$

$$M_{31} \sim \frac{3\sqrt{3/2}}{2\sqrt{q}} + O\left(\frac{1}{q}\right), \quad (62)$$

$$M_{33} \sim 36 + O\left(\frac{1}{q^{1/2}}\right). \quad (63)$$

Then, using Eq. (51), we arrive at

$$\lambda_1 \sim \frac{1}{8q} \quad \text{for } n = 0. \quad (64)$$

Thus, the $n = 0$ soliton is also stable (as it must be since it is the lowest energy stationary state). Curiously, while all of the other solitons' smallest normal mode frequencies are $O(\chi^{3/2})$, the ground state's lowest lying normal mode frequency is actually $O(\chi^2)$ since $\omega_1 = \sqrt{\lambda_1/q} \sim O(\chi^2)$.

VII. CONCLUSIONS

We have shown that the GGPE for the HMF model admits exact solutions in the form of Mathieu functions complemented by a self-consistency condition on the depth of the Hartree potential they generate. These solutions can be

boosted to finite speeds (providing the phase associated with the flow satisfies the periodic boundary conditions). In the strong coupling regime ($\chi \ll 1$) the solutions can be arbitrarily highly localized, and thus we interpret them as bright solitons. A linear stability analysis in the same strong coupling regime shows that they are stable against perturbations when the interactions are attractive.

The fact that the solutions: (1) arise in a periodic potential, (2) are localized, and (3) come in towers with increasing numbers of nodes, means that they have properties in common with gap solitons [137]. However, the periodic potential in the HMF case is self-generated, whereas in the standard gap soliton case the periodic potential is imposed externally. Furthermore, in contrast to the bright soliton solutions of the standard GPE which are stabilized by a $|\psi|^2\psi$ nonlinearity, the HMF model's solitons are stabilized by a nonlocal nonlinearity $\Phi[\psi](\theta) = M[\psi] \cos \theta$, where the depth is given by the magnetization $M[\psi]$; see Eq. (5b).

The approach followed in this work not only allows us to identify solitary wave solutions, but also to find and classify all possible stationary states for both attractive and repulsive interactions at arbitrary coupling strength (we focused on the attractive case). Furthermore, in the strong coupling limit the self-consistency condition can be developed analytically in an asymptotic series so as to provide a completely explicit analytic solution. Given that exact solutions of nonlinear models are few and far between, this illustrates once again that the HMF model is rather special even though it is not thought to be integrable.

One possible reason for the existence of a richer family of solutions (i.e., the tower of solutions) in comparison to the standard short-range attractive system, where the GPE supports a single nodeless bright soliton [i.e., the fundamental soliton given in Eq. (4)], is that the self-consistency condition in the latter case is much more restrictive: both the depth and shape must match. By contrast, in the HMF case the mean-field potential is generated by the coherent addition of the microscopic cosine (XY) interactions and thus inherits a cosine form where only the depth needs to be self-consistently determined. We conjecture that this coherent addition across the sample is a generic feature of LRIs and suggests that such systems deserve closer examination as a potential setting for solitons.

An interesting future direction of research would be to study collisional properties of the bright solitons (solitary waves) identified in this work and to determine if they are true solitons (i.e., do they collide elastically). As sketched in the introduction, systems with LRI can be expected to behave similarly to integrable systems. A numerical study of soliton dynamics in the HMF model would be a natural testing ground for this idea.

Another extension of the present work concerns the quantum phase transition predicted by the HMF model's GGPE due to a spontaneous breaking of translational invariance at the critical value of $\chi = \sqrt{2}$ [116]. The GGPE does not include the effects of quantum fluctuations, and these may inhibit this spontaneous symmetry breaking. However, our exact solutions can serve as the building blocks of more sophisticated quantum states that are required for studying the

role of quantum fluctuations. These effects will be discussed elsewhere [146].

ACKNOWLEDGMENTS

We thank Dmitry Pelinovsky, Robert Dingwall, Wyatt Kirkby, and Thomas Bland for helpful discussions. This research was funded by the Natural Sciences and Engineering Research Council of Canada (NSERC) and the Government of Ontario. Support is also acknowledged from the Perimeter Institute for Theoretical Physics. Research at the Perimeter Institute is supported by the Government of Canada through the Department of Innovation, Science and Economic Development and by the Province of Ontario through the Ministry of Research and Innovation.

APPENDIX A: ASYMPTOTIC ANALYSIS OF THE SELF-CONSISTENT MAGNETIZATION

We are interested in calculating the magnetization

$$\begin{aligned} M_n(\chi) &= \int_{-\pi}^{\pi} d\theta |\psi_n(\theta; \chi)|^2 \cos \theta \\ &= \int_{-\pi}^{\pi} d\theta |\psi_n(\theta; \chi)|^2 \left(1 - 2 \sin^2 \frac{\theta}{2}\right) \\ &= 1 - 2 \int_{-\pi}^{\pi} d\theta |\psi_n(\theta; \chi)|^2 \sin^2 \frac{\theta}{2} \end{aligned}$$

in the strong coupling regime where $\chi \ll 1$. We must consider the cases of n even and n odd separately due to their definition in terms of either even or odd Mathieu functions, which we repeat here for convenience:

$$\psi_n(\theta; \chi, \aleph) = \frac{1}{\sqrt{\pi}} \begin{cases} \text{ce}_n\left[\frac{\theta-\pi}{2}; q_n(\chi; \aleph)\right] & n \text{ even} \\ \text{se}_{n+1}\left[\frac{\theta-\pi}{2}; q_n(\chi; \aleph)\right] & n \text{ odd.} \end{cases} \quad (\text{A1})$$

The strong coupling regime is equivalent to $q \gg 1$ in the conventional Mathieu equation. When applied to the HMF model, this means that one can study the regime in which $q \gg 1$, compute the magnetization and by extension $\chi(q) = \sqrt{4M(q)/q}$, and then invert this expression to find how q depends on χ .

Consequently, it is convenient for computational purposes to consider q , rather than χ as a fixed parameter, and later invert the relationship between them as described above. Integrals such as Eq. (A1) are conveniently analyzed by transforming to the coordinate $\zeta = 2q^{1/4} \sin \frac{\theta}{2}$; doing so we find [as in Eq. (21)]

$$M_n(q) = 1 - \frac{1}{2\sqrt{q}} \int_{-2q^{1/4}}^{2q^{1/4}} \frac{d\zeta}{q^{1/4}} |\psi_n(\zeta; q)|^2 \frac{\zeta^2}{\sqrt{1 - \frac{\zeta^2}{4\sqrt{q}}}}. \quad (\text{A2})$$

For the purposes of obtaining an asymptotic series in $1/\sqrt{q}$ we can extend the limits of integration to $\pm\infty$,

$$M_n(q) \sim 1 - \frac{1}{2\sqrt{q}} \int_{-\infty}^{\infty} \frac{d\zeta}{q^{1/4}} |\psi_n(\zeta; q)|^2 \frac{\zeta^2}{\sqrt{1 - \frac{\zeta^2}{4\sqrt{q}}}}, \quad (\text{A3})$$

where \sim denotes an asymptotically small error as $q \rightarrow \infty$ [122]. We can then expand the square root in the denominator

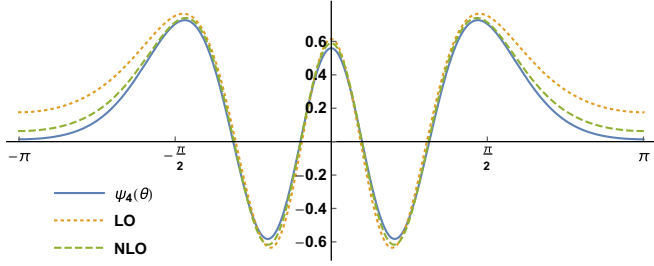


FIG. 6. Comparison of the $n = 4$ exact solitary wave $\psi_n(\theta, q)$ for $q = \frac{2}{3}(2n+1)^2 = 54$. LO denotes the leading-order Sips expansion Eqs. (A4) and (A5), and NLO denotes the approximation including next-to-leading order terms. As we can see, the Sips expansion becomes accurate even at only moderately large values of q . For $q = (2n+1)^2 = 81$ the exact and NLO curves become virtually indistinguishable.

in a Taylor series and use the large- q behavior of the stationary solutions $\psi_n(\zeta; q)$.

In the limit of large q both $ce_n(z; q)$ and $se_n(z; q)$ can be expanded in terms of parabolic cylinder functions [122, 141–144]. This is easy to understand, since for n fixed and $q \rightarrow \infty$ the classical turning points coalesce at the minimum of the cosine potential. Therefore the states are constrained to live arbitrarily close to the potential's minimum and a harmonic approximation is justified. To ensure that the turning point structure is maintained the expansion is carried out using $\xi = 2q^{1/4} \cos z$ rather than the naive choice of $z - \pi/2$. Explicitly, Sips's expansion of the Mathieu functions in terms of parabolic cylinder functions assumes the form [122]

$$ce_n(z; q) \sim \widehat{C}_n(q) [\widehat{U}_n(\xi; q) + \widehat{V}_n(\xi; q)], \quad (\text{A4})$$

$$se_{n-1}(z; q) \sim \widehat{S}_n(q) \sin(z) [\widehat{U}_n(\xi; q) - \widehat{V}_n(\xi; q)], \quad (\text{A5})$$

where $U_m(\xi; q)$ and $V_m(\xi; q)$ are given at next-to-leading order [i.e., suppressing terms of $O(q)$] by

$$\widehat{U}_n(\xi; q) \sim D_n(\xi) + \frac{1}{64\sqrt{q}} \left[\frac{n!}{(n-4)!} D_{n-4}(\xi) - D_{n+4}(\xi) \right], \quad (\text{A6})$$

$$\widehat{V}_n(\xi; q) \sim \frac{1}{16\sqrt{q}} [n(1-n)D_{n-2}(\xi) - D_{n+2}(\xi)], \quad (\text{A7})$$

where $D_n = D_n(\xi)$ are the parabolic cylinder functions of order n , and the normalization constants are given by

$$\widehat{C}_n(q) \sim \left[\frac{\pi\sqrt{q}}{2(n!)^2} \right]^{1/4} \left[1 + \frac{(2n+1)}{8\sqrt{q}} + O\left(\frac{1}{q}\right) \right]^{-1/2}, \quad (\text{A8})$$

$$\widehat{S}_n(q) \sim \left[\frac{\pi\sqrt{q}}{2(n!)^2} \right]^{1/4} \left[1 - \frac{(2n+1)}{8\sqrt{q}} + O\left(\frac{1}{q}\right) \right]^{-1/2}. \quad (\text{A9})$$

The accuracy of the Sips expansion even for relatively modest values of q is illustrated in Fig. 6.

Since we have a series solution to $\psi_n(\zeta; q)$ in terms of parabolic cylinder functions, and we are interested in computing integrals $\int |\psi_n|^2 \zeta^k d\zeta$, we ultimately require knowledge of integrals of the form

$$I_{m,n}^{(k)} = \int_{-\infty}^{\infty} D_m(\xi) D_n(\xi) \xi^k d\xi. \quad (\text{A10})$$

Then using the recursion relation [144]

$$I_{m,n}^{(k)} = I_{m+1,n}^{(k-1)} + I_{m,n+1}^{(k-1)} - (k-1)I_{m,n}^{(k-2)}, \quad (\text{A11})$$

we arrive at the following identities:

$$I_{m,n}^{(0)} = n! \sqrt{2\pi} \times \delta_{m,n}, \quad (\text{A12})$$

$$I_{m,n}^{(1)} = n! \sqrt{2\pi} \times [(n+1)\delta_{m,n+1} + \delta_{m+1,n}], \quad (\text{A13})$$

$$I_{m,n}^{(2)} = n! \sqrt{2\pi} \times [(n+2)(n+1)\delta_{m,n+2} + (2n+1)\delta_{m,n} + \delta_{m+2,n}], \quad (\text{A14})$$

$$I_{n,n}^{(4)} = n! \sqrt{2\pi} \times 3(2n^2 + 2n + 1). \quad (\text{A15})$$

Armed with these details, we may now attack the integral in Eq. (A3). First, we note that by Eq. (A1) that in using Eqs. (A4) and (A5) we must make the substitution $z \rightarrow (\theta + \pi)/2$, which in turn implies that $\xi \rightarrow \zeta = 2q^{1/4} \sin(\theta/2)$ and $\sin z \rightarrow \cos(\theta/2)$. Expressing all functions in terms of ζ and then performing a Taylor expansion yields

$$M_n(q) \sim 1 - \int_{-\infty}^{\infty} \frac{d\zeta}{q^{1/4}} \left[\frac{1}{\sqrt{\pi}} \right]^2 [\widehat{U}_n(\zeta) \pm \widehat{V}_n(\zeta)]^2 \left[\left(\frac{\pi\sqrt{q}}{2(n!)^2} \right)^{1/4} \right]^2 \left(1 \mp \frac{2n+1}{8\sqrt{q}} \right) \times \left(\frac{1}{2\sqrt{q}} \zeta^2 \pm \frac{1}{16q} \zeta^4 \right), \quad (\text{A16})$$

where the upper sign corresponds to n even and the lower sign to n odd. Using Eqs. (A12) to (A14), the integral may then be expressed in terms of $I_{m,n}^{(k)}$ as

$$\begin{aligned} M_n(q) &\sim 1 - \frac{1}{n! \sqrt{2\pi}} \left\{ \frac{1}{2\sqrt{q}} I_{n,n}^{(2)} \pm \frac{1}{16q} [I_{n,n}^{(4)} + n(1-n)I_{n,n-2}^{(2)} - I_{n,n+2}^{(2)} - (2n+1)I_{n,n}^{(2)}] \right\} + O\left(\frac{1}{q^{3/2}}\right) \\ &= 1 - \frac{1}{2\sqrt{q}} [2n+1] \mp \frac{1}{16q} [3(2n^2 + 2n + 1) + n(1-n) - (n+1)(n+2) - (2n+1)^2] + O\left(x \frac{1}{q^{3/2}}\right) \\ &= 1 - \frac{1}{2\sqrt{q}} [2n+1] + O\left(\frac{1}{q^{3/2}}\right). \end{aligned} \quad (\text{A17})$$

Having obtained the magnetization in terms of the auxiliary parameter q , we now compute $\chi(q)$ and find at next-to-next-to-leading order

$$\chi(q_n) = \sqrt{\frac{4M_n(q)}{q}} \sim \frac{2}{\sqrt{q}} \left[1 - \frac{1}{\sqrt{q}} \frac{2n+1}{4} - \frac{1}{q} \frac{(2n+1)^2}{32} \right], \quad (\text{A18})$$

which may in turn be inverted to find

$$q_n(\chi; \aleph = 1) \sim \frac{4}{\chi^2} \left[1 - \frac{2n+1}{4} \chi - \frac{(2n+1)^2}{32} \chi^2 \right] \quad (\text{A19})$$

as claimed in the main text. The branch labeled by $\aleph = 1$ is the appropriate one since we took the auxiliary variable q to be large.

APPENDIX B: DEFINITION AND ASYMPTOTICS OF THE INTEGRALS $\mathcal{I}_{m,n}^C$ AND $\mathcal{I}_{m,n}^S$

The following integrals appear in Eq. (36):

$$\mathcal{I}_{m,n}^C = \int_{-\pi}^{\pi} \phi_m(\theta) \psi_n(\theta) \cos \theta \, d\theta, \quad (\text{B1})$$

$$\mathcal{I}_{m,n}^S = \int_{-\pi}^{\pi} \phi_m(\theta) \psi_n(\theta) \sin \theta \, d\theta, \quad (\text{B2})$$

where ψ_n is the stationary state [given by a Mathieu function with depth parameter $q(\chi)$] around which fluctuations take place, and ϕ_m is a Mathieu function orthogonal⁵ to ψ_m .

Note that both ψ_n and ψ_m , being Mathieu functions, are strictly even or odd, and so $\mathcal{I}_{m,n}^C = 0$ identically if $m+n$ is odd, while $\mathcal{I}_{m,n}^S = 0$ identically if $m+n$ is even. We can compute these integrals order-by-order in $1/\sqrt{q}$ by re-expressing them in terms of $\zeta = 2q^{1/4} \sin \frac{\theta}{2}$. For the sine integral we find

$$\begin{aligned} \mathcal{I}_{m,n}^S &= \int_{-2q^{1/4}}^{2q^{1/4}} \left[\frac{d\zeta}{q^{1/4} \left(1 - \frac{\zeta^2}{4\sqrt{q}}\right)} \right] \phi_m(\zeta; q) \psi_n(\zeta; q) \\ &\times \left[\frac{\zeta}{q^{1/4}} \sqrt{1 - \frac{\zeta^2}{4\sqrt{q}}} \right]. \end{aligned} \quad (\text{B3})$$

⁵The functions $\{\psi_m\}$ satisfy the (rescaled) linear Mathieu equation $-\frac{\chi^2}{2} \phi_m'' - M[\psi_n] \cos \theta \phi_m = \lambda_m \phi_m$.

Next, using the asymptotic formulas for Mathieu functions, Eqs. (A4) and (A5), and working at leading order in $1/\sqrt{q}$ we find

$$\begin{aligned} \mathcal{I}_{m,n}^S &\sim \int_{-2q^{1/4}}^{2q^{1/4}} d\zeta \frac{\zeta}{\sqrt{q}} \left\{ \frac{1}{\sqrt{\pi}} \left[\frac{\pi\sqrt{q}}{2(n!)^2} \right]^{1/4} D_n(\zeta) \right\} \\ &\times \left\{ \frac{1}{\sqrt{\pi}} \left[\frac{\pi\sqrt{q}}{2(m!)^2} \right]^{1/4} D_m(\zeta) \right\} \\ &= \frac{1}{q^{1/4}} \frac{1}{\sqrt{2\pi m!n!}} I_{n,m}^{(1)} \\ &= \frac{1}{q^{1/4}} [\sqrt{n+1} \delta_{m,n+1} + \sqrt{n} \delta_{m+1,n}], \end{aligned} \quad (\text{B4})$$

where we have made use of Eq. (A13) to move between the second and third equalities. For Eq. (48) we require $\mathcal{I}_{m,n}^S$ with $m = n \pm 1$ at next-to-leading order, to calculate $\delta\mathcal{F}$. These are given by

$$\mathcal{I}_{n+1,n}^S = q^{1/4} \left[\sqrt{n+1} - \frac{3(n+1)}{8\sqrt{q}} \right], \quad (\text{B5})$$

$$\mathcal{I}_{n-1,n}^S = q^{1/4} \left[n - \frac{3n}{8\sqrt{q}} \right]. \quad (\text{B6})$$

Next, turning our attention to the cosine integral we find

$$\begin{aligned} \mathcal{I}_{m,n}^C &= \int_{-2q^{1/4}}^{2q^{1/4}} \left[\frac{d\zeta}{q^{1/4} \left(1 - \frac{\zeta^2}{4\sqrt{q}}\right)} \right] \phi_m(\zeta; q) \psi_n(\zeta; q) \\ &\times \left[1 - \frac{\zeta^2}{2\sqrt{q}} \right]. \end{aligned} \quad (\text{B7})$$

When re-expressed in terms of parabolic cylinder functions, we see that the $O(1)$ piece vanishes ($\int D_m D_n d\zeta = 0$ for $m \neq n$), and the remaining integral ($\int D_m D_n \zeta^2 / \sqrt{q} d\zeta$) is $O(1/\sqrt{q})$. This implies that

$$I_{m,n}^C \sim O\left(\frac{1}{\sqrt{q}}\right). \quad (\text{B8})$$

This is subdominant to the sine integral $I_{m,n}^S \sim O(1/q^{1/4})$ and so can be neglected at leading order as claimed in the main text.

- [1] J. S. Russell, Report on waves, *Report of the 14th Meeting of the British Association for the Advancement of Science*, York (John Murray, London, 1844), pp. 311–390.
- [2] P. G. Drazin and R. S. Johnson, *Solitons: An Introduction* (Cambridge University Press, Cambridge, 1989).
- [3] M. Tanaka, The stability of solitary waves, *Phys. Fluids* **29**, 650 (1986).
- [4] Z. Wang, Stability and dynamics of two-dimensional fully nonlinear gravity-capillary solitary waves in deep water, *J. Fluid Mech.* **809**, 530 (2016).
- [5] W. Y. Duan, Z. Wang, B. B. Zhao, R. C. Ertekin, and J. W. Kim, Steady solution of the velocity field of steep solitary waves, *Appl. Ocean Res.* **73**, 70 (2018).

- [6] L. F. Mollenauer, R. H. Stolen, and J. P. Gordon, Experimental Observation of Picosecond Pulse Narrowing and Solitons in Optical Fibers, *Phys. Rev. Lett.* **45**, 1095 (1980).
- [7] J. P. Gordon, Interaction forces among solitons in optical fibers, *Opt. Lett.* **8**, 596 (1983).
- [8] Y. Kodama and K. Nozaki, Soliton interaction in optical fibers, *Opt. Lett.* **12**, 1038 (1987).
- [9] A. Hasegawa, *Optical Solitons in Fibers* (Springer, Berlin, 1989).
- [10] Y. S. Kivshar and B. Luther-Davies, Dark optical solitons: Physics and applications, *Phys. Rep.* **298**, 81 (1998).
- [11] L. F. Mollenauer and J. P. Gordon, *Solitons in Optical Fibers* (Academic Press, New York, 2006).

- [12] K. E. Strecker, G. B. Partridge, A. G. Truscott, and R. G. Hulet, Formation and propagation of matter-wave soliton trains, *Nature (London)* **417**, 150 (2002).
- [13] L. Khaykovich, F. Schreck, G. Ferrari, T. Bourdel, J. Cubizolles, L. D. Carr, Y. Castin, and C. Salomon, Formation of a matter-wave bright soliton, *Science* **296**, 1290 (2002).
- [14] S. L. Cornish, S. T. Thompson, and C. E. Wieman, Formation of Bright Matter-Wave Solitons during the Collapse of Attractive Bose-Einstein Condensates, *Phys. Rev. Lett.* **96**, 170401 (2006).
- [15] A. L. Marchant, T. P. Billam, T. P. Wiles, M. M. H. Yu, S. A. Gardiner, and S. L. Cornish, Controlled formation and reflection of a bright solitary matter-wave, *Nat. Commun.* **4**, 1865 (2013).
- [16] G. D. McDonald, C. C. N. Kuhn, K. S. Hardman, S. Bennetts, P. J. Everitt, P. A. Altin, J. E. Debs, J. D. Close, and N. P. Robins, Bright Solitonic Matter-Wave Interferometer, *Phys. Rev. Lett.* **113**, 013002 (2014).
- [17] P. Medley, M. A. Minar, N. C. Cizek, D. Berryrieser, and M. A. Kasevich, Evaporative Production of Bright Atomic Solitons, *Phys. Rev. Lett.* **112**, 060401 (2014).
- [18] S. Burger, K. Bongs, S. Dettmer, W. Ertmer, K. Sengstock, A. Sanpera, G. V. Shlyapnikov, and M. Lewenstein, Dark Solitons in Bose-Einstein Condensates, *Phys. Rev. Lett.* **83**, 5198 (1999).
- [19] J. Denschlag, J. E. Simsarian, D. L. Feder, C. W. Clark, L. A. Collins, J. Cubizolles, L. Deng, E. W. Hagley, K. Helmerson, W. P. Reinhardt, S. L. Rolston, B. I. Schneider, and W. D. Phillips, Generating solitons by phase engineering of a Bose-Einstein condensate, *Science* **287**, 97 (2000).
- [20] Z. Dutton, M. Budde, C. Slowe, and L. V. Hau, Observation of quantum shock waves created with ultra-compressed slow light pulses in a Bose-Einstein condensate, *Science* **293**, 663 (2001).
- [21] G.-B. Jo, J.-H. Choi, C. A. Christensen, T. A. Pasquini, Y.-R. Lee, W. Ketterle, and D. E. Pritchard, Phase-Sensitive Recombination of Two Bose-Einstein Condensates on an Atom Chip, *Phys. Rev. Lett.* **98**, 180401 (2007).
- [22] P. Engels and C. Atherton, Stationary and Nonstationary Fluid Flow of a Bose-Einstein Condensate through a Penetrable Barrier, *Phys. Rev. Lett.* **99**, 160405 (2007).
- [23] A. Weller, J. P. Ronzheimer, C. Gross, J. Esteve, M. K. Oberthaler, D. J. Frantzeskakis, G. Theocharis, and P. G. Kevrekidis, Experimental Observation of Oscillating and Interacting Matter Wave Dark Solitons, *Phys. Rev. Lett.* **101**, 130401 (2008).
- [24] S. Stellmer, C. Becker, P. Soltan-Panahi, E.-M. Richter, S. Dörscher, M. Baumert, J. Kronjäger, K. Bongs, and K. Sengstock, Collisions of Dark Solitons in Elongated Bose-Einstein Condensates, *Phys. Rev. Lett.* **101**, 120406 (2008).
- [25] J. J. Chang, P. Engels, and M. A. Hoefer, Formation of Dispersive Shock Waves by Merging and Splitting Bose-Einstein Condensates, *Phys. Rev. Lett.* **101**, 170404 (2008).
- [26] C. Becker, S. Stellmer, P. Soltan-Panahi, S. Dörscher, M. Baumert, E.-M. Richter, J. Kronjäger, K. Bongs, and K. Sengstock, Oscillations and interactions of dark and dark-bright solitons in Bose-Einstein condensates, *Nat. Phys.* **4**, 496 (2008).
- [27] C. Hamner, J. J. Chang, P. Engels, and M. A. Hoefer, Generation of Dark-Bright Soliton Trains in Superfluid-Superfluid Counterflow, *Phys. Rev. Lett.* **106**, 065302 (2011).
- [28] A. C. Scott, F. Y. F. Chu, and D. W. McLaughlin, The soliton: A new concept in applied science, *Proc. IEEE* **61**, 1443 (1973).
- [29] A. Scott, *Nonlinear Science: Emergence and Dynamics of Coherent Structures* (Oxford University Press, Oxford, 2003).
- [30] C. Klein and J.-C. Saut, IST versus PDE, a comparative study, [arXiv:1409.2020](https://arxiv.org/abs/1409.2020) (2014).
- [31] M. Hudak, J. Tothova, and O. Hudak, Inverse scattering method I. Methodological part with an example: Soliton solution of the Sine-Gordon equation, doi: [10.13140/RG.2.2.35000.65287](https://doi.org/10.13140/RG.2.2.35000.65287).
- [32] C. J. Pethick and H. Smith, *Bose-Einstein Condensation in Dilute Gases* (Cambridge University Press, Cambridge, 2002).
- [33] R. C. Davidson, *Physics of Nonneutral Plasmas* (World Scientific, Singapore, 2001).
- [34] F. Calogero, Solution of the one-dimensional n-body problem with quadratic and/or inversely quadratic pair potentials, *J. Math. Phys.* **12**, 419 (1971).
- [35] B. Sutherland, Exact results for a quantum many-body problem in one dimension, *Phys. Rev. A* **4**, 2019 (1971).
- [36] B. Sutherland, Exact results for a quantum many-body problem in one dimension. II, *Phys. Rev. A* **5**, 1372 (1972).
- [37] L. Santos, G. V. Shlyapnikov, P. Zoller, and M. Lewenstein, Bose-Einstein Condensation in Trapped Dipolar Gases, *Phys. Rev. Lett.* **85**, 1791 (2000).
- [38] A. Griesmaier, J. Werner, S. Hensler, J. Stuhler, and T. Pfau, Bose-Einstein Condensation of Chromium, *Phys. Rev. Lett.* **94**, 160401 (2005).
- [39] T. Lahaye, T. Koch, B. Fröhlich, M. Fattori, J. Metz, A. Griesmaier, S. Giovanazzi, and T. Pfau, Strong dipolar effects in a quantum ferrofluid, *Nature (London)* **448**, 672 (2007).
- [40] T. Koch, T. Lahaye, J. Metz, B. Fröhlich, A. Griesmaier, and T. Pfau, Stabilization of a purely dipolar quantum gas against collapse, *Nat. Phys.* **4**, 218 (2008).
- [41] Q. Beaufils, R. Chicireanu, T. Zanon, B. Laburthe-Tolra, E. Maréchal, L. Vernac, J.-C. Keller, and O. Gorceix, All-optical production of chromium Bose-Einstein condensates, *Phys. Rev. A* **77**, 061601(R) (2008).
- [42] T. Lahaye, C. Menotti, L. Santos, M. Lewenstein, and T. Pfau, The physics of dipolar bosonic quantum gases, *Rep. Prog. Phys.* **72**, 126401 (2009).
- [43] M. Lu, N. Q. Burdick, S. H. Youn, and B. L. Lev, Strongly Dipolar Bose-Einstein Condensate of Dysprosium, *Phys. Rev. Lett.* **107**, 190401 (2011).
- [44] K. Aikawa, A. Frisch, M. Mark, S. Baier, A. Rietzler, R. Grimm, and F. Ferlaino, Bose-Einstein Condensation of Erbium, *Phys. Rev. Lett.* **108**, 210401 (2012).
- [45] N. I. Nikolov, D. Neshev, O. Bang, and W. Z. Królikowski, Quadratic solitons as nonlocal solitons, *Phys. Rev. E* **68**, 036614 (2003).
- [46] W. Królikowski, O. Bang, N. I. Nikolov, J. Wyller, J. J. Rasmussen, and D. Edmundson, Modulational instability, solitons and beam propagation in spatially nonlocal nonlinear media, *J. Opt. B* **6**, S288 (2004).
- [47] N. I. Nikolov, D. Neshev, W. Królikowski, O. Bang, J. J. Rasmussen, and P. L. Christiansen, Attraction of nonlocal dark optical solitons, *Opt. Lett.* **29**, 286 (2004).

- [48] Q. Kong, Q. Wang, and W. Królikowski, Analytical theory of dark nonlocal solitons, *Opt. Lett.* **35**, 2152 (2010).
- [49] W. Chen, M. Shen, Q. Kong, J. Shi, Q. Wang, and W. Królikowski, Interactions of nonlocal dark solitons under competing cubic-quintic nonlinearities, *Opt. Lett.* **39**, 1764 (2014).
- [50] A. Dreischuh, D. N. Neshev, D. E. Petersen, O. Bang, and W. Królikowski, Observation of Attraction between Dark Solitons, *Phys. Rev. Lett.* **96**, 043901 (2006).
- [51] C. Conti, A. Fratallocchi, M. Peccianti, G. Ruocco, and S. Trillo, Observation of a Gradient Catastrophe Generating Solitons, *Phys. Rev. Lett.* **102**, 083902 (2009).
- [52] A. P. Polychronakos, Waves and Solitons in the Continuum Limit of the Calogero-Sutherland Model, *Phys. Rev. Lett.* **74**, 5153 (1995).
- [53] I. Andrić, V. Bardek, and L. Jonke, Solitons in the Calogero-Sutherland collective-field model, *Phys. Lett. B* **357**, 374 (1995).
- [54] D. Sen and R. K. Bhaduri, Applications of the collective field theory for the Calogero-Sutherland model, *Ann. Phys.* **260**, 203 (1997).
- [55] V. Bardek, J. Feinberg, and S. Meljanac, Density waves in the Calogero model—Revisited, *Ann. Phys.* **325**, 691 (2010).
- [56] M. J. Edmonds, T. Bland, D. H. J. O'Dell, and N. G. Parker, Exploring the stability and dynamics of dipolar matter-wave dark solitons, *Phys. Rev. A* **93**, 063617 (2016).
- [57] P. Pedri and L. Santos, Two-Dimensional Bright Solitons in Dipolar Bose-Einstein Condensates, *Phys. Rev. Lett.* **95**, 200404 (2005).
- [58] J. Cuevas, B. A. Malomed, P. G. Kevrekidis, and D. J. Frantzeskakis, Solitons in quasi-one-dimensional Bose-Einstein condensates with competing dipolar and local interactions, *Phys. Rev. A* **79**, 053608 (2009).
- [59] B. B. Baizakov, S. M. Al-Marzoug, and H. Bahlouli, Interaction of solitons in one-dimensional dipolar Bose-Einstein condensates and formation of soliton molecules, *Phys. Rev. A* **92**, 033605 (2015).
- [60] K. Pawłowski and K. Rzazewski, Dipolar dark solitons, *New J. Phys.* **17**, 105006 (2015).
- [61] T. Bland, M. J. Edmonds, N. P. Proukakis, A. M. Martin, D. H. J. O'Dell, and N. G. Parker, Controllable nonlocal interactions between dark solitons in dipolar condensates, *Phys. Rev. A* **92**, 063601 (2015).
- [62] A. Triay, Derivation of the dipolar Gross-Pitaevskii energy, *SIAM J. Math. Anal.* **50**, 33 (2018).
- [63] A. Eychenne and N. Rougerie, On the stability of 2D dipolar Bose-Einstein condensates [arXiv:1809.07085](https://arxiv.org/abs/1809.07085) (2018).
- [64] M. J. Ablowitz and Z. H. Musslimani, Integrable nonlocal nonlinear equations, *Stud. Appl. Math.* **139**, 7 (2017).
- [65] M. Ablowitz, I. Bakirtas, and B. Ilan, Wave collapse in a class of nonlocal nonlinear Schrödinger equations, *Physica D* **207**, 230 (2005).
- [66] S. V. Manakov, On the theory of two-dimensional stationary self-focusing of electromagnetic waves, *Zh. Eksp. Teor. Fiz.* **65**, 505 (1973) [*Sov. Phys.-JETP* **38**, 248 (1974)].
- [67] P. G. Kevrekidis and D. J. Frantzeskakis, Solitons in coupled nonlinear Schrödinger models: A survey of recent developments, *Rev. Phys.* **1**, 140 (2016).
- [68] S. G. Evangelides, L. F. Mollenauer, J. P. Gordon, and N. S. Bergano, Polarization multiplexing with solitons, *J. Lightwave Technol.* **10**, 28 (1992).
- [69] P. K. A. Wai and C. R. Menyuk, Polarization decorrelation in optical fibers with randomly varying birefringence, *Opt. Lett.* **19**, 1517 (1994).
- [70] J. Yang, Physically significant nonlocal nonlinear Schrödinger equation and its soliton solutions, *Phys. Rev. E* **98**, 042202 (2018).
- [71] R. A. Van Gorder, Quantum Hasimoto transformation and nonlinear waves on a superfluid vortex filament under the quantum local induction approximation, *Phys. Rev. E* **91**, 053201 (2015).
- [72] P. Jetzer, Boson stars, *Phys. Rep.* **220**, 163 (1992).
- [73] F. E. Schunck and E. W. Mielke, General relativistic boson stars, *Class. Quantum Grav.* **20**, R301 (2003).
- [74] E. Seidel and W.-M. Suen, Formation of Solitonic Stars through Gravitational Cooling, *Phys. Rev. Lett.* **72**, 2516 (1994).
- [75] S. Khlebnikov, Short-scale gravitational instability in a disordered Bose gas, *Phys. Rev. D* **62**, 043519 (2000).
- [76] A. Elgart and B. Schlein, Mean field dynamics of boson stars, *Commun. Pure Appl. Math.* **60**, 500 (2007).
- [77] P. Sikivie and Q. Yang, Bose-Einstein Condensation of Dark Matter Axions, *Phys. Rev. Lett.* **103**, 111301 (2009).
- [78] O. Erken, P. Sikivie, H. Tam, and Q. Yang, Cosmic axion thermalization, *Phys. Rev. D* **85**, 063520 (2012).
- [79] H.-Y. Schive, T. Chiueh, and T. Broadhurst, Cosmic structure as the quantum interference of a coherent dark wave, *Nat. Phys.* **10**, 496 (2014).
- [80] D. G. Levkov, A. G. Panin, and I. I. Tkachev, Relativistic Axions from Collapsing Bose Stars, *Phys. Rev. Lett.* **118**, 011301 (2017).
- [81] D. G. Levkov, A. G. Panin, and I. I. Tkachev, Gravitational Bose-Einstein Condensation in the Kinetic Regime, *Phys. Rev. Lett.* **121**, 151301 (2018).
- [82] I. M. Moroz, R. Penrose, and P. Tod, Spherically-symmetric solutions of the Schrödinger-Newton equations, *Class. Quantum Grav.* **15**, 2733 (1998).
- [83] M. Bahrami, A. Großardt, S. Donadi, and A. Bassi, The Schrödinger-Newton equation and its foundations, *New J. Phys.* **16**, 115007 (2014).
- [84] D. O'Dell, S. Giovanazzi, G. Kurizki, and V. M. Akulin, Bose-Einstein Condensates with $1/r$ Interatomic Attraction: Electromagnetically Induced “Gravity,” *Phys. Rev. Lett.* **84**, 5687 (2000).
- [85] S. Giovanazzi, G. Kurizki, I. E. Mazets, and S. Stringari, Collective excitations of a “gravitationally” self-bound Bose gas, *Europhys. Lett.* **56**, 1 (2001).
- [86] M. Antoni and S. Ruffo, Clustering and relaxation in Hamiltonian long-range dynamics, *Phys. Rev. E* **52**, 2361 (1995).
- [87] M. Kac, G. E. Uhlenbeck, and P. C. Hemmer, On the van der Waals theory of the vapor-liquid equilibrium. I. Discussion of a one-dimensional model, *J. Math. Phys.* **4**, 216 (1963).
- [88] T. Dauxois, V. Latora, and A. Rapisarda, The Hamiltonian mean field model: From dynamics to statistical mechanics and back, *Dynamics and Thermodynamics of Systems with Long-Range Interactions*, Lecture Notes in Physics, Vol. 602 (Springer, Berlin, 2002), pp. 458–487.
- [89] A. Campa, T. Dauxois, and S. Ruffo, Statistical mechanics and dynamics of solvable models with long-range interactions, *Phys. Rep.* **480**, 57 (2009).

- [90] Y. Levin, R. Pakter, F. B. Rizzato, Ta. N. Teles, and F. P. C. Benetti, Nonequilibrium statistical mechanics of systems with long-range interactions, *Phys. Rep.* **535**, 1 (2014).
- [91] S. Schütz and G. Morigi, Prethermalization of Atoms Due to Photon-Mediated Long-Range Interactions, *Phys. Rev. Lett.* **113**, 203002 (2014).
- [92] A. T. Black, H. W. Chan, and V. Vuletić, Observation of Collective Friction Forces due to Spatial Self-Organization of Atoms: From Rayleigh to Bragg Scattering, *Phys. Rev. Lett.* **91**, 203001 (2003).
- [93] K. Baumann, C. Guerlin, F. Brennecke, and T. Esslinger, Dicke quantum phase transition with a superfluid gas in an optical cavity, *Nature (London)* **464**, 1301 (2010).
- [94] R. Mottl, F. Brennecke, K. Baumann, R. Landig, T. Donner, and T. Esslinger, Roton-type mode softening in a quantum gas with cavity-mediated long-range interactions, *Science* **336**, 1570 (2012).
- [95] J. Léonard, A. Morales, P. Zupancic, T. Esslinger, and T. Donner, Supersolid formation in a quantum gas breaking a continuous translational symmetry, *Nature (London)* **543**, 87 (2017).
- [96] J. G. Cosme, C. Georges, A. Hemmerich, and L. Mathey, Dynamical Control of Order in a Cavity-BEC System, *Phys. Rev. Lett.* **121**, 153001 (2018).
- [97] R. M. Kroeze, Y. Guo, V. D. Vaidya, J. Keeling, and B. L. Lev, Spinor Self-Ordering of a Quantum Gas in a Cavity, *Phys. Rev. Lett.* **121**, 163601 (2018).
- [98] S. Schütz, S. B. Jäger, and G. Morigi, Thermodynamics and dynamics of atomic self-organization in an optical cavity, *Phys. Rev. A* **92**, 063808 (2015).
- [99] S. Schütz, S. B. Jäger, and G. Morigi, Dissipation-Assisted Prethermalization in Long-Range Interacting Atomic Ensembles, *Phys. Rev. Lett.* **117**, 083001 (2016).
- [100] T. Keller, S. B. Jäger, and G. Morigi, Phases of cold atoms interacting via photon-mediated long-range forces, *J. Stat. Mech.* (2017) 064002.
- [101] T. Keller, V. Torggler, S. B. Jäger, S. Schütz, H. Ritsch, and G. Morigi, Quenches across the self-organization transition in multimode cavities, *New J. Phys.* **20**, 025004 (2018).
- [102] J. Binney and S. Tremaine, *Galactic Dynamics* (Princeton University Press, Princeton, 2011).
- [103] D. Lynden-Bell, Statistical mechanics of violent relaxation in stellar systems, *Mon. Not. R. Astron. Soc.* **136**, 101 (1967).
- [104] Y. Y. Yamaguchi, One-dimensional self-gravitating sheet model and Lynden-Bell statistics, *Phys. Rev. E* **78**, 041114 (2008).
- [105] R. Pakter and Y. Levin, Core-Halo Distribution in the Hamiltonian Mean-Field Model, *Phys. Rev. Lett.* **106**, 200603 (2011).
- [106] T. Dauxois, P. Holdsworth, and S. Ruffo, Violation of ensemble equivalence in the antiferromagnetic mean-field XY model, *Eur. Phys. J. B* **16**, 659 (2000).
- [107] F. Leyvraz, M.-C. Firpo, and S. Ruffo, Violation of ensemble equivalence in the antiferromagnetic mean-field XY model, *J. Phys. A* **35**, 4413 (2002).
- [108] J. Barré, F. Bouchet, T. Dauxois, and S. Ruffo, Out-of-Equilibrium States as Statistical Equilibria of an Effective Dynamics in a System with Long-Range Interactions, *Phys. Rev. Lett.* **89**, 110601 (2002).
- [109] J. Barré, F. Bouchet, T. Dauxois, and S. Ruffo, Birth and long-time stabilization of out-of-equilibrium coherent structures, *Eur. Phys. J. B* **29**, 577 (2002).
- [110] J. Ye, S. Sachdev, and N. Read, Solvable Spin Glass of Quantum Rotors, *Phys. Rev. Lett.* **70**, 4011 (1993).
- [111] T. K. Kopeć, Infinite-range-interaction M -component quantum spin glasses: Statics and dynamics in the large- M limit, *Phys. Rev. B* **50**, 9963 (1994).
- [112] N. Read, S. Sachdev, and J. Ye, Landau theory of quantum spin glasses of rotors and Ising spins, *Phys. Rev. B* **52**, 384 (1995).
- [113] M. P. Kennett, C. Chamon, and J. Ye, Aging dynamics of quantum spin glasses of rotors, *Phys. Rev. B* **64**, 224408 (2001).
- [114] S. Sachdev, *Quantum Phase Transitions* (Cambridge University Press, Cambridge, 2011).
- [115] P.-H. Chavanis, The quantum HMF model: I. Fermions, *J. Stat. Mech.* (2011) P08002.
- [116] P.-H. Chavanis, The quantum HMF model: II. Bosons, *J. Stat. Mech.* (2011) P08003.
- [117] R. Plestid, P. Mahon, and D. H. J. O'Dell, Violent relaxation in quantum fluids with long-range interactions, *Phys. Rev. E* **98**, 012112 (2018).
- [118] W. Braun and K. Hepp, The Vlasov dynamics and its fluctuations in the $1/n$ limit of interacting classical particles, *Commun. Math. Phys.* **56**, 101 (1977).
- [119] S. Ogawa and Y. Y. Yamaguchi, Linear response theory in the Vlasov equation for homogeneous and for inhomogeneous quasistationary states, *Phys. Rev. E* **85**, 061115 (2012).
- [120] A. Patelli and S. Ruffo, General linear response formula for non integrable systems obeying the Vlasov equation, *Eur. Phys. J. D* **68**, 329 (2014).
- [121] L. Pitaevskii and S. Stringari, *Bose-Einstein Condensation*, International Series of Monographs on Physics (Clarendon Press, Oxford, 2003).
- [122] G. Wolf, Mathieu functions and Hills equation, in *NIST Handbook of Mathematical Functions*, edited by F. W. J. Olver, D. W. Lozier, R. F. Boisvert, and C. W. Clark (Cambridge University Press, Cambridge, 2010), Vol. 5, p. 966.
- [123] B. Prasanna Venkatesh, M. Trupke, E. A. Hinds, and D. H. J. O'Dell, Atomic Bloch-Zener oscillations for sensitive force measurements in a cavity, *Phys. Rev. A* **80**, 063834 (2009).
- [124] B. Prasanna Venkatesh, J. Larson, and D. H. J. O'Dell, Band-structure loops and multistability in cavity QED, *Phys. Rev. A* **83**, 063606 (2011).
- [125] B. P. Venkatesh and D. H. J. O'Dell, Bloch oscillations of cold atoms in a cavity: Effects of quantum noise, *Phys. Rev. A* **88**, 013848 (2013).
- [126] H. Keßler, J. Klinder, B. Prasanna Venkatesh, Ch. Georges, and A. Hemmerich, *In situ* observation of optomechanical Bloch oscillations in an optical cavity, *New J. Phys.* **18**, 102001 (2016).
- [127] Ch. Georges, J. Vargas, H. Keßler, J. Klinder, and A. Hemmerich, Bloch oscillations of a Bose-Einstein condensate in a cavity-induced optical lattice, *Phys. Rev. A* **96**, 063615 (2017).
- [128] M. D. Lee, S. D. Jenkins, Y. Bronstein, and J. Ruostekoski, Stochastic electrodynamics simulations for collective atom response in optical cavities, *Phys. Rev. A* **96**, 023855 (2017).

- [129] J. Goldwin, B. P. Venkatesh, and D. H. J. O'Dell, Backaction-Driven Transport of Bloch Oscillating Atoms in Ring Cavities, *Phys. Rev. Lett.* **113**, 073003 (2014).
- [130] M. Samoylova, N. Piovella, G. R. M. Robb, R. Bachelard, and Ph. W. Courteille, Synchronization of Bloch oscillations by a ring cavity, *Opt. Express* **23**, 14823 (2015).
- [131] M. Coles and D. Pelinovsky, Loops of energy bands for Bloch waves in optical lattices, *Stud. Appl. Math.* **128**, 300 (2012).
- [132] B. Eiermann, Th. Anker, M. Albiez, M. Taglieber, P. Treutlein, K.-P. Marzlin, and M. K. Oberthaler, Bright Bose-Einstein Gap Solitons of Atoms with Repulsive Interaction, *Phys. Rev. Lett.* **92**, 230401 (2004).
- [133] B. Wu and Q. Niu, Nonlinear Landau-Zener tunneling, *Phys. Rev. A* **61**, 023402 (2000).
- [134] J. C. Bronski, L. D. Carr, B. Deconinck, and J. N. Kutz, Bose-Einstein Condensates in Standing Waves: The Cubic Nonlinear Schrödinger Equation with a Periodic Potential, *Phys. Rev. Lett.* **86**, 1402 (2001).
- [135] B. Wu and Q. Niu, Superfluidity of Bose-Einstein condensate in an optical lattice: Landau-Zener tunnelling and dynamical instability, *New J. Phys.* **5**, 104 (2003).
- [136] M. Machholm, C. J. Pethick, and H. Smith, Band structure, elementary excitations, and stability of a Bose-Einstein condensate in a periodic potential, *Phys. Rev. A* **67**, 053613 (2003).
- [137] P. J. Y. Louis, E. A. Ostrovskaya, C. M. Savage, and Y. S. Kivshar, Bose-Einstein condensates in optical lattices: Band-gap structure and solitons, *Phys. Rev. A* **67**, 013602 (2003).
- [138] M. Machholm, A. Nicolin, C. J. Pethick, and H. Smith, Spatial period doubling in Bose-Einstein condensates in an optical lattice, *Phys. Rev. A* **69**, 043604 (2004).
- [139] J. Satsuma and N. Yajima, Initial value problems of one-dimensional self-modulation of nonlinear waves in dispersive media, *Prog. Theor. Phys. Supp.* **55**, 284 (1974).
- [140] V. E. Zakharov and A. B. Shabat, Exact theory of two-dimensional self-focusing and one-dimensional self-modulation of waves in nonlinear media, *Sov. Phys. JETP* **34**, 62 (1972).
- [141] R. Sips, Representation asymptotique des fonctions de Mathieu et des fonctions d'onde spheroidales, *Trans. Am. Math. Soc.* **66**, 93 (1949).
- [142] R. Sips, Représentation asymptotique des fonctions de Mathieu et des fonctions sphéroidales. II, *Trans. Am. Math. Soc.* **90**, 340 (1959).
- [143] R. B. Dingle and H. J. W. Müller, Asymptotic expansions of Mathieu functions and their characteristic numbers, *J. Reine Angew. Math.* **211**, 11 (1962).
- [144] D. Frenkel and R. Portugal, Algebraic methods to compute Mathieu functions, *J. Phys. A* **34**, 3541 (2001).
- [145] Y. Castin, Bose-Einstein condensates in atomic gases: Simple theoretical results, in *Coherent Atomic Matter Waves*, edited by R. Kaiser, C. Westbrook, and F. David (Springer, Berlin, 2001), pp. 1–136.
- [146] R. Plestid and J. Lambert (unpublished).